Stockholm University

Master Thesis

Degree Project in Geochemistry 45 hp

A study on Dissolved Methane in the Water Column at an Inshore Site in the Baltic Sea

Transport or in situ generation?

Jonas Fredriksson

Stockholm 2019

Department of Geological Sciences
Stockholm University
SE-106 91 Stockholm

The Aim

Adaequatio intellectus et rei.

-Thomas Aquinas

The Road

Cuiusvis hominis est errare, nullius nisi insipientis in errore perseverare.

-Cicero

The End

Scribimus indocti doctique poemata passim.

-Horace

A study on Dissolved Methane in the Water Column at an Inshore Site in the Baltic Sea.

Transport or in situ generation?

Abstract

Methane maxima in oxic waters of the upper water column have been found in oceans and lakes around the world. In this study we explored a brack-water site in the Trosa archipelago in the western parts of the Baltic Sea. This site exhibits enhanced surface concentrations of dissolved methane and hosts numerous seep sites with gases of with unknown composition, possibly containing thermogenic methane.

We studied the concentration of methane and its isotopic composition, $\delta^{13}C$, in the sediments, the benthic boundary layer, and the water column. And tracked the changes during the spring and summer months. In addition, we used a benthic lander system with several sensors, amongst them and acoustic Doppler profiler and a benthic bubble trap, to try to understand and create an integrated view of the water movement and sediment-water interaction of this complex near shore site.

We found, based on arguments of isotope mixing, that the main contributor to the methane flux to the atmosphere was methane which had been produced in situ in the upper waters. And that neither the contributions from diffusion of a biogenic sedimentary source nor ebullition of biogenic or abiotic methane could constitute the lion share of the flux. From current and meteorological data, we also found it very unlikely that lateral transport could play any significant part. We also show how the complex nature and swift changes of the current regime in this region and the water mass interaction with the sea floor necessitates concurrent current and concentration measurements and that extrapolations and assumptions regarding turbulent flow based on a “log law of the wall” argument does not hold.

Table of Contents

A study on Dissolved Methane in the Water Column at an Inshore Site in the Baltic Sea. 2
Transport or in situ generation? 2
Abstract 2
Introduction 5
General Introduction 5
Theoretical background 6
The Water Column: Physical properties, transport, and atmospheric exchange. 7
The Benthic Boundary Layer (BBL) and sediment water exchange 8
The Sediments 10
Pathways for methanogenesis 10
Aim of study 10
Methods 12
Overview 12
Planned and executed deployments and sampling runs 13
In situ measurements and sample retrieval 14
Water column proper 14
The Benthic boundary layer and the topmost sediments 14
Sediments 16
Sediment cores for incubation 16
Sediment cores for methane concentration 17
Lab analysis and postprocessing 17
Methane concentration 17
Methane isotope analysis 19
Alkalinity 20
Results 22
Water Column CTD 22
Water Column 23
The Benthic Boundary Layer 23
Benthic CTD data 24
Benthic boundary Layer Water Velocity Profiles May 16th 27
Benthic boundary Layer Water Velocity Profiles August 6th 28
Benthic Boundary Layer Water Properties Time Series 29
Temperature and Velocity Anomaly 30
Methane Concentration 31
δ13C-CH4 32
Comparing alkalinity and dissolved methane for DET and and normal water sampling. 33

Discussion....34
BBL water data....34
On the trustworthiness of Method....34
Methane....35
Local or transported....35
Ebullitions....36
Two upper water column sources?....36
A strong thermogenic source?....36
Conclusions....37
Acknowledgements....37
Bibliography....38
Appendix....42
$\delta^{13}C$ response relative to peak area for the GC/Isolink IRMS....42
Comments regarding the deployments.....42
Core Incubation....44
Discussing a Failed Core Incubation Experiment....45
Search for the lost lander....46

Introduction

General Introduction

Methane is the smallest of the hydrocarbons and a potent greenhouse gas. It is nearly ubiquitous both in the universe at large as well as on earth. It can be created through both abiotic processes as well as through biologically mediated reactions. The biologically mediated processes can be divided into three main groups, i.e. 1) fermentation, 2) reduction of carbon dioxide, and 3) de-methylation of various methyl compounds such as methyl phosphate, dimethylsulfoniopropionate (DMSP), or methylamine (Lovley and Klug, 1983). Examples of abiotic pathways would be thermogenic methane and serpentinization reactions (see Galimov, 1974; Kreulen and Schuiling, 1982; Schoell, 1988, and a summary by Etiope, 2017). Thermogenic methane is associated with the formation of natural gas and serpentinization reactions are important weathering reactions near mid-ocean ridges and at hydrothermal vents (Welhan, 1981). The end product in all these cases is a molecule consisting of one carbon and 4 covalently bonded hydrogen atoms. However, it is possible to distinguish and trace the origin of a methane sample by utilizing the fact that both hydrogen and carbon have more than one naturally occurring stable isotope. The various methanogenic reactions differ in their isotope fractionation and permit tracing of the formation pathway (see Stahl, 1977; Fuex, 1977; Lebedev et al., 1969 and also Schoell, 1988). Stevens (1988) tracked the trends of atmospheric emissions using isotope ratios. Other examples to distinguish between specific biotic pathways such as between fermentation and carbon dioxide reduction have been shown, e.g. Whiticar et al., 1986 in a lacustrine environment. In both lacustrine and marine systems methanogenesis is intimately tied to the carbon cycle. The photic layer of the water column serve as a carbon sink where dissolved CO_2 is incorporated into biomass by photo-synthesis. Carbon bound in biomass is then recycled and remineralised in situ or transported to the sea floor where it undergoes further decomposition. The decomposition is driven by the availability of electron acceptors and usually follows a general order, i.e. oxygen is consumed first followed by nitrate, manganese, iron, and sulphate (Froelich et al., 1979). The reason is that microbes exploiting higher energy-yielding pathways will generally be able to outcompete microbes that use less energetically favourable electron acceptors. When all non-carbon electron acceptors have been consumed methanogens will take over through the process of reduction of carbon dioxide or fermentation. These are by far the least energetically favourable metabolic pathways. The biologically produced methane produced accumulates in the sediments, but also escape the sediments through slow diffusion or ebullition back into the water column. Methane production is generally associated with anoxic sediments since the methanogens tend to be outcompeted in oxic environments by other microbes which use more energetically favourable pathways and because the methanogenic pathways are inhibited by oxygen (e.g. Cheng et al, 2008).

However, several researchers, e.g. Brooks and Sacket 1973, 1977; Scranton and Brewer 1977; Scranton and Farrington 1977; Brooks et al. 1981, have observed a methane concentration maximum in oxygen-rich water column associated with the pycnocline, effectively decoupled from a sediment source. This methane concentration maximum has been associated with biological activity, e.g. Lamontagne et al., 1973; Scranton and Brewer, 1977; and Brooks et al., 1981, and it has been hypothesised (Scranton and Brewer, 1977; Sieburth et al., 1987; Oremland, 1979) that production occurs in anoxic diffusion-limited microenvironments

which defined by Burke et al. (1987) as: “inside dead cells, fecal pellets or the guts of larger organisms; or in association with nitrogen-fixing bacteria or algae”. They assumed the existence of these micro-environments because the fermentation and carbon dioxide reduction methanogenic pathways are severely inhibited by the presence of oxygen. In fact, two recent studies have found a link between both methanogenesis in the gut of copepods (Schmale et al., 2017) and as a biproduct of nitrogen fixation in the bacterium Rhodopseudomonas palustris (Zheng, 2018). Xiao et al)2017) have also found evidence of concurrent methane production and oxidation in oxic sediments. It is also possible that archaeal methanogens can be active in these environments by using a substrate to feed on that is less favourable to other microbes such as methanol, methylamines and some organic sulphur compounds (Kiene et al., 1986; Marty, 1992). Methane production in oxic surface waters has been shown to be greatest when and where the primary productivity is high, such as in upwelling regions, where saturation levels of 200% have been observed (Owens et al., 1991) , but has also been tied to dimethylsulfoniopropionate (DMSP) availability and correlated with chlorophyll-a concentrations (Damm et al., 2008). These oceanic and freshwater systems have been explored since the late 1970’s. An intermediate, but under explored, system that exhibits similar elevated methane signals are that of brackish water bodies. The Baltic Sea being shallow, heavily eutrophic as well as the second largest brackish water sea in the world would make an excellent choice for exploring these processes in a brack water setting. The eutrophication of the Baltic Sea ensures a high amount of primary productivity associated with abundant secondary consumers, high carbon export to the sea floor, and carbon-rich sediments. The general shallow water depth of the Baltic Sea allows for efficient -low mass loss- transport of ebullitive methane originating in the sediments, advectively transported dissolved methane in the water column in addition to the potential for in situ methanogenesis in the upper water column. All in all, the Baltic Sea is an under-explored setting that is capable of supporting a wide range of methanogen pathways, geological and biological methane sources, and transport vectors. In order to patch this gap in our knowledge, i.e. the origin and transport of methane in the photic zone of large brackish waters, the problem will be further explored at a site in the Baltic Sea.

Theoretical background

When studying the sediment-water-atmosphere system it is necessary to subdivide the system into several distinct systems with the division based on their inherent properties and to focus on the processes in the layers, the exchange between them and the different sampling methods required to probe them. For this project the chosen division was to consider 1) **the sediments** (where particulate matter originating in the water column is deposited; remineralisation takes place; and CO_2, CH_4, and nutrients are recharged into the benthic boundary layer), 2) **the benthic boundary** layer (where waterflow is affected by shear stress induced by the sediment surface, and 3) **the water column proper** stretching from above the benthic boundary layer to the surface (where water flows freely, mixes due to wind and waves, and where physical gradients develop).

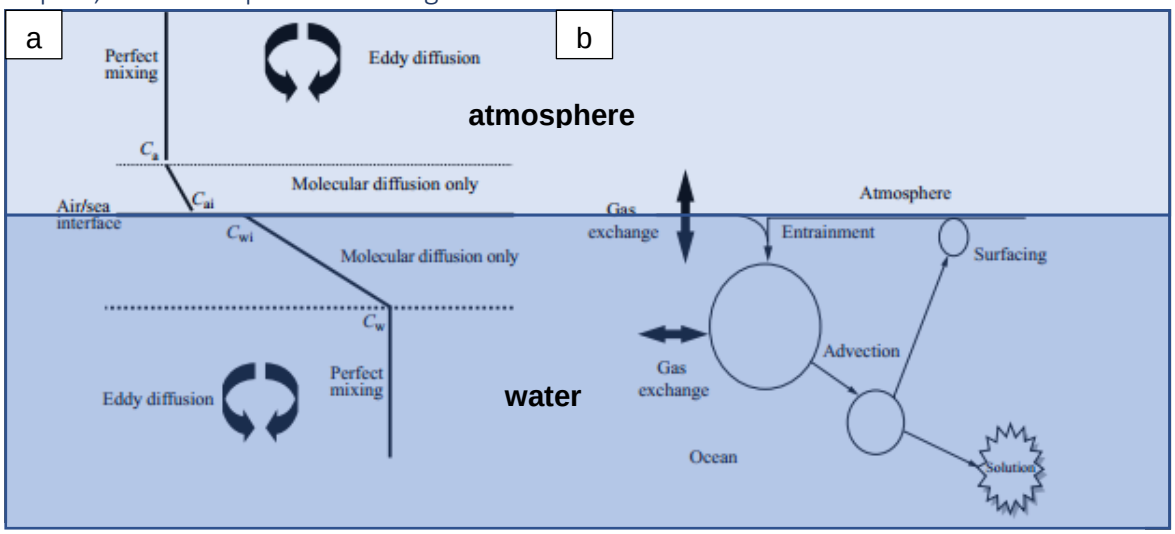

Figure 1: Two models of water atmosphere exchange. a) at low windspeeds where the exchange is limited by molecular diffusion and where the thickness of the diffusive boundary layer is depending on wind speed..b) at higher windspeeds breaking waves will entrap bubbles effectively increasing the surface area through which diffusion takes place. Reproduced from Liss and Slater, 1974 (a) and Woolf, 1997 (b).

The photic mixed surface zone is where primary productivity takes place and which serves as a sink of carbon dioxide as the carbon from the carbon dioxide is taken up and incorporated into biomass by primary producers. Globally the recycling of elements in this zone is very efficient as the net primary productivity of the oceans is 45-50 Pg. C/year but with only 1 Pg. C is tied up in biomass at any one time (Falkowski *et al*., 1998). The particulate matter that doesn't get recycled collates, forms aggregates and sinks through the water column, through the BBL, releasing nutrients and DIC as it is slowly degraded during the transport, eventually ending up on the sediment surface. Phytoplankton can also indirectly affect the physical properties of the water column. They will, during phytoplankton blooms, scatter and absorb light in the photic zone which may enhance warming of the surface water and initiate the formation of a thermocline (Townsend *et al*. 1992). A well-developed thermocline will divide the water column and inhibit advective transport and turbulent mixing of solutes and dissolved gases but not hinder bubble transport. Thermoclines are also associated with pycnoclines, which are the interfaces, where the density increases, and suspended particles can accumulate. It is also where zooplankton resides during daytime to avoid feeding pressure by fish in surface waters (Lampert, 1989).

The degradation of particulate matter as it sinks is mirrored by the consumption of high energy reduced carbon released from the sediments, i.e. methane. The concentration of methane decreases upwards in the water column, away from its sediment source, due to the source distance, turbulent mixing (dilution) and microbial consumption. The oxidation by methanotrophs changes the isotopic signature of methane, from the strong negative signature associated with methanogenesis towards a heavier isotopic signature (Whiticar, 1999).

Dissolved gases in the upper waters will strive to reach thermodynamic equilibrium with the atmosphere but will be limited by the exchange rate across the water surface. Away from the surface the mixing of gases is effective and driven by turbulent diffusion. However, near the surface a diffusive boundary layer (DBL) is formed which limits the exchange rate with the atmosphere (Wanninkhof, 1992), which

produces enhanced concentrations of dissolved gases relative to atmospheric equilibrium in surface waters. The water-atmosphere exchange rate is greatly enhanced when the wind is strong enough to create breaking waves since this mixes the water and entrains bubbles; effectively increasing the surface area through which diffusion takes place (see also Liss and Slater, 1974; and Woolf, 1997).

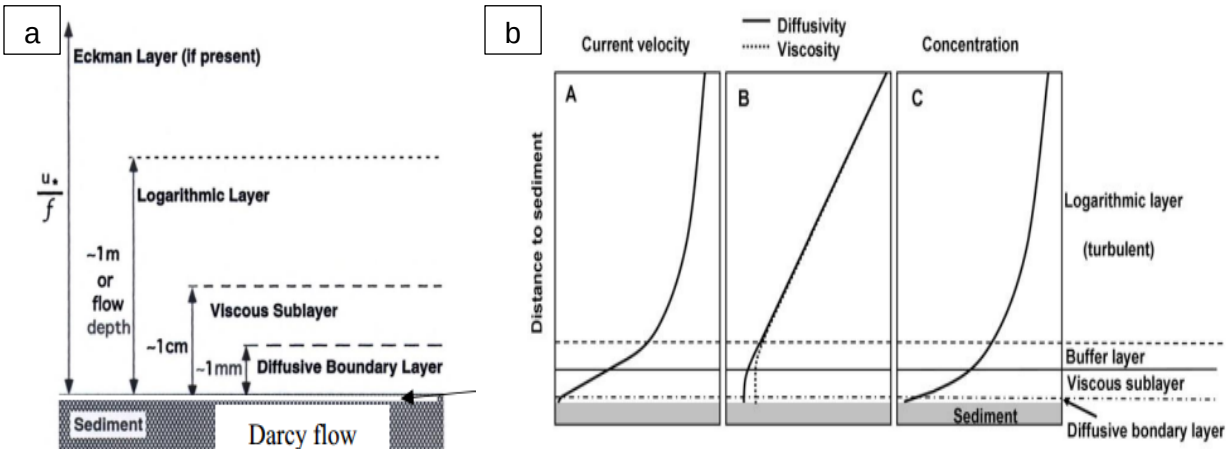

Figure 2: Schematic idealised divisions of the benthic boundary layer. The left picture shows the approximate sizes of the layers in a low flow regime (a). The right picture, b, shows a schematic of the benthic boundary layer with the interrelation of current velocity, diffusivity-viscosity, and solute concentration for a solute with a sink in sediments (e.g. oxygen). Reproduced from Boudreau and Jørgensen, 2001 (a) and Holtappels, 2009 (b).

The Benthic Boundary Layer (BBL) and sediment water exchange

The Benthic Boundary Layer (BBL) consists of the lowest part of the water column. It is located where the water column transits into the sediments surface. The interaction between the moving water column and stationary sediment surface induces shear stress and increases mixing due to turbulent diffusion. This shear stress can also cause resuspension and lateral transport of sediments and keep sinking particles in suspension due to the shear induced turbulence (Thomson and Graf, 1994, van Weering et al., 2001). This is also where the concentrations of dissolved inorganic electron acceptors (O_2, NO_3^-, SO_4^{2-}) are high, availability of reduced carbon is plentiful, and the nutrient concentrations are high since they are recharged from the sediments. The availability of nutrients and the strong redox potential can be utilised by microbes, whose abundance is enhanced relative to that of the water column (Ritzrau and Thomsen, 1997). The remineralisation rates in the BBL can be high enough to rival those in the sediments (Thomsen et al., 2002). It is hard to precisely define the height at which the benthic boundary layer ends since the upper boundary is also dependent on current velocity. A convention is that the BBL ends when the water velocity reaches 99% of the free flow velocity (Pope, 2000). For flow-velocities of 1-15 cm this height can vary between 2-20 m (Dade *et al*. 2001).

At an idealised sediment surface the flow velocity is by definition zero. In the absence of bioturbation and bioirrigation, transport across this layer is driven by molecular diffusion obeying Fick's law of diffusion. Farther away the flow is viscous with a velocity gradient dependent on viscous stress. In this layer turbulence can be regarded to be negligible. The layer above sees increased, non-negligible, Reynold's stress and is a transition layer into the region farthest from the seafloor where the flow is turbulent and increases with the eddy size scaling almost linearly with the distance from the sediments (Boudreau, 2001) and the velocity increasing

logarithmically with the distance from the sea floor (von Karman, 1930), see figure 2. For a more extensive discussion of the various layers and their physical properties see also Pope (2000). However, as the illustration in figure 3 shows, there are multiple processes that can affect the flow of both particulates and solutes across the sediment-water interface. E.g. shear driven flow, Darcy flow and the activity of burrowers, figure 2, and 3.

By analysing the concentrations just above the sediment surface, i.e. within the diffusive boundary layer, the diffusive flux out of or into the sediments can be calculated (Jørgensen and Revsbech, 1985). Farther above the sediments it is possible to describe turbulent transport using a quasi-Fick:ian law of diffusion, with diffusion coefficients orders of magnitude higher than that of molecular diffusion. These increase with distance from the seabed and can be used to determine fluxes across the sediment-water interface with knowledge of the concentration gradients and the turbulent diffusivity. This treatment will also integrate contributions from lateral sources into the total flux (see discussion in Holtappels and Lorke (2011). Another method includes core incubation which can be used to determine the oxygen flux (Glud et al., 1994). This can then be used together with concentration measurements in the BBL to determine fluxes of other solutes from their gradients. This method yields the total flux and accounts for the components of diffusive flux and bioirrigation if the incubated area is large enough (Berg et al. 2007). The area that contributes to the near, 0.05 to 0.3 m above, the sediments can be estimated based on the sediment roughness parameter, independent on current velocity (berg et al., 2007)

The benthic boundary layer is unreachable by shipboard means, it cannot be sampled by a wire operated CTD nor can water samples be reliably retrieved from a ship-based system. Sediment cores have been the preferred method of remote sampling of this region. An in-situ method of collecting data and samples from this region is by employing a benthic lander system.

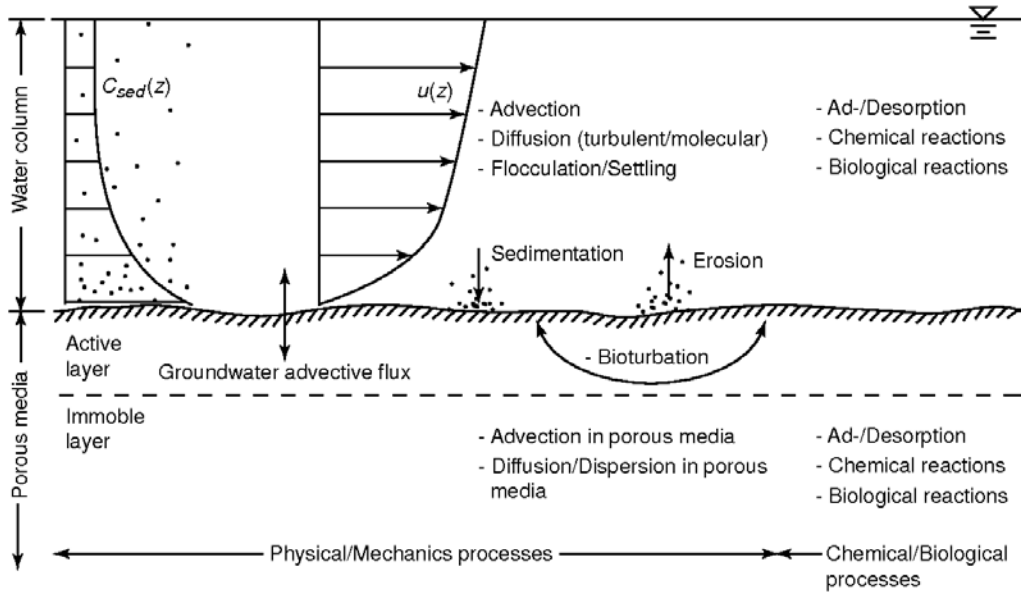

Figure 3: Schematic overview of the processes affecting flux across the sediment-water interface. (Boundary Exchange, 2005).

The Sediments

The sediments are the final sink of particulate matter. Here carbon is re-mineralised and either trapped or resuspended back in to the water column via the benthic boundary layer. The sediments can be characterised by the availability of oxidised inorganic compounds that microbes use in their metabolism as electron acceptors. It has been shown that there is an order in the redox reactions (e.g. Froelich et al., 1979; Reeburgh, 1980). In the upmost millimetre oxygen is used as an electron acceptor (Jørgensen, 1982) followed by nitrate-, iron- manganese-, and sulphate-reduction. In the last stages, when all other electron acceptors are used up, carbon itself is used, both as an electron acceptor and donor, in fermentation processes or by reduction of CO_2 (Stumm and Morgan, 1981). These last anoxic processes yield methane and are mediated by Archaea. The sequential order of these reactions in the sediments is largely driven by energy yield of the reactions, e.g. it is well established that sulphate reducers outcompete methanogens when both are present and compete for the same electron donor (see e.g. Abram and Nedwell, 1978). However, coexistence of methanogens and sulphate reducers is possible for non-competitive substrates such as the case of methanol and methylamines which are favoured by methanogens but not by sulphate reducers (e.g. Oremland et al., 1982).

The methane (as well as the other rest-products of metabolism and released nutrients) can then be transported from the sediments. The transport in fine-grained permeable clays and muds by diffusion is slow. The presence of burrowing micfrofauna mixes the sediments and provides bio-irrigation which increases the advective transport into the sediments, changes the magnitude of released nutrient fluxes and changes the physical properties of the sediments (Reichfelt, 1991).

Pathways for methanogenesis

There are several known biological pathways for metabolically driven methanogenesis all of which are mediated by archaea. In addition to these there are non-metabolic biological pathways such as methylotrophic methanogenesis. In short, the metabolical pathways can be described using redox reactions were we either have reduction of carbon dioxide

$$4H_2 + CO_2 \rightarrow CH_4 + 2H_2O$$

or acetoclastic methanogenesis

$$CH_3COOH \rightarrow CH_4 + CO_2$$

(Conrad, 2005). Both metabolic pathways are severely inhibited by the presence of oxygen (Storz et al., 1990; Schönheit et al., 1981). In both cases the reactants used are products from bacterial metabolism. There are also several studies that hint at methane production in oxic environments using demethylation pathways. An example would be demethylation of dimethylsulfoniopropionate (DMSP). Another recently discovered pathway is tied to nitrogen fixation and has been shown for the nitrogen-fixing bacterium Rhodopseudomonas palustris which, in the same enzymatic step, reduces carbon dioxide together with nitrogen gas and protons to yield methane, ammonia, and dihydrogen (Zheng et al., 2018).

Aim of study

In this study we aim to study methane at a site which exhibits enhanced atmospheric and high water column methane concentrations, as well as multiple ebullition sites in the Trosa archipelago. Following in the footsteps of and expanding upon the work done by Fanny Axelsson in this area 2017. The aim of the study was therefore to establish whether the water column methane distribution could be explained by sedimentary sources in the underlying sediments, explained by lateral transport, or by production higher up in the water column.

The purpose of the study was to determine the concentration and carbon isotope composition ($\delta^{13}C$) of the methane in the sediments, the benthic boundary layer, and the water column. Sediments were sampled by retrieving sediment cores and through passive sampling. The transition into the benthic boundary layer was studied by retrieving water samples with high spatial resolution using a benthic lander system. The water column was sampled using Niskin bottles. In addition, in order to have a better understanding of the physical properties of the water column physical data was also collected (over periods of days to weeks) from the benthic boundary layer using a benthic lander system. This included measurements of: temperature, salinity, turbidity, dissolved oxygen, and current velocities.

My hypothesis was that the elevated methane is due to local production and does not originate from the sediments. Rather that it is produced in the water column and can be tied to biological activity related to algal blooms. If true, this would enhance our source-flux understanding of methane in any eutrophic brack water setting.

Methods

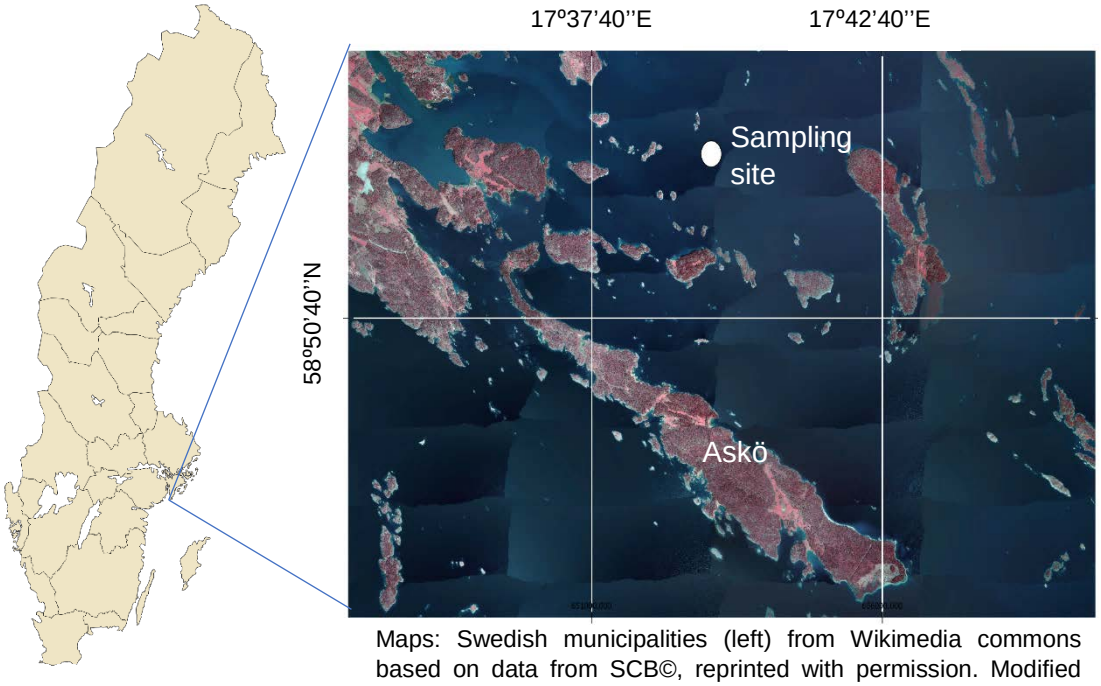

Maps: Swedish municipalities (left) from Wikimedia commons based on data from SCB©, reprinted with permission. Modified DEM of Askö ©Lantmäteriet 2018. WGS84.

Figure 4: Sampling site. North of the island Askö in the Trosa archipelago. All sampling took place at the marked position.

Overview

The sampling site was situated north of the island Askö in the Fifångsdeep in the Trosa Archipelago (figure 4, also see appendix for a bathymetric map). The water depth at the different deployment localities varied between 24 and 26 meters and the sea floor topography was generally flat. The sediment stratigraphy can be described to consist of till followed by glacial clays, postglacial clays, and more recent muds, all overlying a deformed and fractured crystalline bedrock. Water column concentrations above the atmospheric equilibrium concentration of methane (1.85 ppm in the atmosphere and correspondingly 3.2 nM in the water column) have been measured during the spring and summer of 2017 (Fanny Axelsson, 2018). In addition, seep sites of unidentified gases have been identified in the region (Jakobsson et al., 2016, Lundmark, 2017) and it has been further speculated that they could contain methane, possibly of thermogenic origin. Thermogenic methane has been found at sites with similar tectonic features in the Stockholm Archipelago (Söderberg and Flodén, 1992)

For sampling purposes, the area of interest was divided into three parts, the water column proper (defined as the part of the water column where water moves in the free flow regime and which can be sampled from a ship), the benthic boundary layer (for practical purposes the 80 cm of the water column directly overlying the sediments), and the sediments (sampled to a depth of about 20 cm). Various methods were used to sample and probe them.

1. **The water column proper** and the mixed surface layer was sampled using a CTD to determine temperature, salinity, turbidity, photosynthetically active radiation (PAR) and dissolved oxygen. Niskin bottles were used to retrieve water samples.
2. **The Benthic Boundary Layer (BBL)** was sampled by a benthic

lander (modelled on a system by Thomsen et al, 1994). The lander was placed on the seafloor and was continually logging CTD data, current flow data, dissolved oxygen as well as retrieving water samples in situ. For a more detailed information on the operation of the lander see Fredriksson, 2017. In addition, a diffusion equilibration sampler (DET) was attached to the lander as well as a camera. A peristaltic pump in association with stationary inlets allowed for high, sub-centimetre, vertical resolution water sampling. With sampling down to a centimetre above the sediment water interface.

3. **The sediments** that were part sampled by equipment attached to the lander and part by retrieving sediment cores which were further analysed in the lab.

To achieve this several deployments were planned with varying goals and success rates.

Planned and executed deployments and sampling runs

Table 1:Deployments, goals, and retrieved data.

Date	**Place**	**Goal**	**Attained**
2017-11-26	Askö-Fifång[1]	• Test Hesslein sampler (DET) • Retrieve sediment core for incubation experiment • Benthic CTD data	Yes Yes Yes
2018-02-15	Askö-Fifång[2]	• Water Column CTD data • Water samples • Lander deployment 2 week. • Sediment core	No No No No
2018-04-05	Askö-Fifång[3]	• Water Column Data • Water samples • Lander deployment 2 week. • Sediment cores • Benthic bubble trap	CTD data No No Yes Yes
2018-05-16	Askö-Fifång[4]	• Water Column CTD data • Water samples • Lander deployment 2 week. • Sediment core • DET data • Benthic bubble trap	Yes Yes Yes Yes No, lost. No, lost.
2018-08-06	Askö-Fifång	• Water Column CTD data • Water samples • Lander deployment 8 days. • DET data • Benthic bubble trap	Yes Yes Yes Yes Yes
2018-08-16	Askö-Fifång	• Water Column CTD data • Water samples • Lander deployment 10 days • DET data	Yes Yes Yes, but long term BBL-CTD data lost. Yes

[1] All deployments were at, or within 100 m of 58 51.3786 N 017 39.1373 E near The Fifång. Deep in the Trosa archipelago north of Askö.
[2] Cancelled due to sudden sea ice growth.
[3] Aborted halfway through due to ice floes.
[4] Lander with all equipment lost while performing long term in situ sampling. Salvaged by The Swedish Royal Navy 7 weeks later.

In situ measurements and sample retrieval

Water column proper

CTD

Basic water properties of the water column were collected and logged using a Sea and Sun CTD with conductivity, temperature, pressure, turbidity, fluorometers, and an optical, fast response time, oxygen sensor (RINKO optode). The CTD was either attached to a wire or mounted on the benthic lander. Data was logged on both descent and ascent of the CTD, but only data collected during the descent was used. During some deployments a LED-light was activated to provide light for a downward-looking GoPro camera. This adversely affected the turbidity sensor allowing only the detection of changes in turbidity rather than absolute values. The turbidity is reported in FTU (Formazin Turbidity Units). The presence of the LED did not affect the PAR measurements. The pressure measured by the CTD's internal pressure sensor was used as a proxy for depth. No compensation for salinity and temperature was performed.

Water samples

Water samples were retrieved using a Niskin bottle. The collected water was carefully poured via a small hose, to minimise bubbles and turbulence, into the bottom of bottles or exetainers. The containers were filled to the brim, capped with rubber caps and gas sealed with septa. Care was taken so that there were no bubbles in the containers. Three sets of water samples were collected for each depth and sampling time: water for $\delta^{13}C$-CH_4, water for CH_4 concentrations, and water for alkalinity determination. The water stored for isotope analysis were stored in 1000 ml Duran® borosilicate bottles sealed with a gas tight rubber cap and those for methane concentration and alkalinity were stored in 12 ml exetainers® with septum caps. The samples were transported in a cool bag and stored at 4 ºC. The gas samples were stored prior to analysis and were poisoned by adding 1 ml 50% $ZnCl_2$ per 10 ml of sample. Some samples that had not been treated with $ZnCl_2$ were lost prior to analysis.

The Benthic boundary layer and the topmost sediments

Water samples

Water from the benthic boundary layer was collected in two stages. First the lander was placed on the sea floor, and the peristaltic pump (12 channels, KC-Denmark) set to start 5 minutes after landing. This was to allow suspended sediments to settle and bottom water disturbed by the

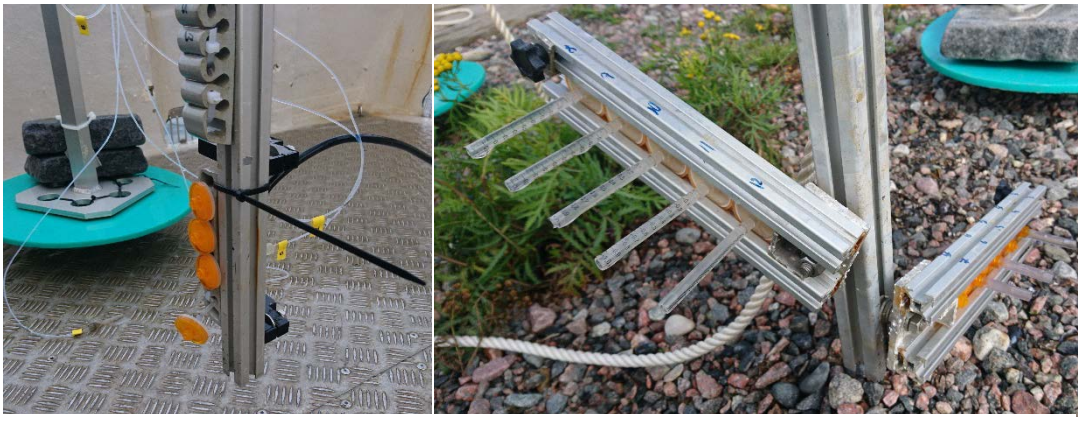

Figure 5: Two inlet solutions for water sampling at the benthic boundary layer. The left picture shows the original setup with the inlets and orange filters attached to a vertical beam. And the right picture shows a setup where the height of sampling can be adjusted by tilting the filter holders and extension to minimise the effect of inlet-holder induced turbulence.

emplacement to be removed by lateral transport. Then the first set of water samples were collected using the peristaltic pump by filling gastight 60 ml SOFT-JECT® syringes, after passing a 0.45 μm filter at the inlet (see figure 5). The lander was then retrieved, and the collected water was carefully transferred, without headspace, into 12 ml exetainers and sealed with rubber septum caps. The syringes were then replaced with Tedlar® bags and the process was repeated. Tedlar® bags were used for their gas-storing properties as well as allowing for greater sample size. However, switching from syringes to Tedlar® bags allowed some air to enter the system. When the Tedlar® bags were retrieved with the water samples they contained a small amount of free gas that was gently squeezed out.

The pump inlet rack was changed during the project to allow for easier use, greater customisation, and minimisation of air entry into the hose system, as well as to reduce the effect of turbulence by the inlets themselves. BBL water samples collected from May and onwards used the setup on the right (figure 5)

CTD

The CTD was attached to a lift with a pre-programmed repeating lift sequence. The sequence started by moving the lift with the attached CTD at the top moving down over 11 depth intervals with a spacing of 10, 10, 10, 10, 5, 5, 5, 1, 1, 1, 1, cm. A complete depth section cycle took about 2.5 hours. The sensor position on the CTD frame prevented the sensor to collect data in the bottommost centimetre closest to the sediment surface. Two additional oxygen sensors (Aanderaa) were attached at fixed positions closer to the sediments. The CTD continuously logged pressure, temperature, salinity, PAR and turbidity.

ADCP

An acoustic Doppler current profiler (Aquadopp, Nortek AS, Bergen, Norway) was mounted looking downward in the interior of the lander frame ~70 cm above the seafloor. The 3-beam setup with a 2 MHz sampling frequency was used to sample ~60 10 mm high cells above the sea floor. The rate of sampling as well as burst sampling setups were tested in attempts to accommodate the demands of high temporal resolution and battery consumption. The settings were:

May
Burst interval: 450 s
Cell size 10 mm
Average interval: 60 s
Blanking distance: 0.1 m
Pulse distance: 0.8 m

August 6th
Burst interval: 60 s
Cell size 10 mm
Average interval: 60 s
Blanking distance: 0.12 m
Pulse distance: 0.795 m

August 16th
Burst sampling with 512 samples and a rate of 1 Hz.
Burst interval: 1200 s
Cell size 8 mm
Blanking distance: 0.1 m
Pulse distance: 0.75 m

Hesslein sampler

Methane in the porewater and the overlying water column was sampled using a passive diffusion sampler. The passive sampler was modelled after R. Hesslein´s in-situ porewater sampler (Hesslein, 1976). The sampler consists of a 20 by 35 cm slab of polyoxymethylene (POM) into which horizontal elongated compartments were milled. The bottom part was sharpened to more easily penetrate the sediments and cause minimal disturbance. POM was the chosen material since it is cheap, easy to process, and for its low diffusivity and permeability (Massey, 2003; Belles et al, 2017). The compartments were placed 1 cm off centre from each other. Slits of the same size and relative location were drilled into a thin cover plate that was attached to

Figure 6: Hesslein sampler. The blue needle is inserted at the top. Water is extracted from the bottom of the slit and transferred to the 6 ml exetainer®. The slit with the blue needle is approximately 2 cm below the sediment-water interface.

the main plate by means of nylon screws. A 0.05 mm thin sheet of B Teflon[5]® with pre-punched holes for the screws, was placed between the slab and the cover plate. The lid and Teflon® sheet were screwed on while submerged in Milli-Q water to ensure that no gas was trapped in the equilibration chambers. To minimise the impact of the chamber water on the sediments the oxygen was removed from the water by addition of sodium sulphite (Na_2SO_3) crystals to the outside of the membrane to allow the consumption of dissolved oxygen in the chamber water.

This sampler was then attached to the lander frame so that part would be inserted into the sediments with the remainder exposed to bottom water. The sampler was left on the lander to equilibrate with its surroundings and retrieved with the lander after 8-14 days. The water in the Hesslein sampler was retrieved by holding it sideways, inserting a needle through the Teflon at the top, and removing the water with a syringe from the bottom (see figure 6). This was to prevent bubbles traversing the sample chamber and scavenging the water of dissolved gases. The retrieved water was then transferred to 6 ml exetainers that were capped, without headspace, with a septum lid.

The positioning of the equilibration sampler chambers overlapped with the sampling inlets collected by the peristaltic pump allowing for comparison of samples from both samplers.

Benthic Bubble Trap

The underwater bubble trap that was deployed consisted of an inverted conical funnel (Ø 24 cm) attached to a flexible silicon hose. The other end of the hose terminated in the bottom part of a 12 ml Exetainer® made of borosilicate with a perforated bottom. The funnel was attached to the outer frame of the benthic lander and with the hose trailing upwards to the ropes ending at the exetainer approximately 4 m above the lander. The system was waterfilled at the time of deployment and bubbles emitted from the sea floor was captured by the funnel, transiting through the hose, and finally accumulating in the exetainer. The accumulated gas was then retrieved by a syringe perforating the septum in the top of the Exetainer®, when the lander was retrieved just before it exited the water. The gas was transferred to another Exetainer® that had been prefilled with NaCl-saturated water. Excess water was removed from the exetainer with a syringe.

Sediments

Sediment cores for incubation

Sediment cores for incubation experiments were retrieved using a multi-corer (Mini Muc K/MT 410, Kiel, Germany). Holding 4 60 cm long 9.5 cm wide core liners. 4 lead weights on the multi-corer were used to adjust the weight and allow penetration of the cores into the sediment The large sediment cores were sub-sampled with smaller core liners that were made of plexiglass, 25 cm high, and 7 cm Ø. The core liners had a contactless optical oxygen

[5] The Teflon (polytetrafluorethylene (PTFE)) was from a virgin (not reprocessed) PTFE resin skived film that had been sintered without additives.

sensor spot (PyroScience GmbH, Aachen, Germany) attached at the upper inside of the cores. Only cores that showed no obvious sign of disturbance of the sediments and clear overlying water were kept. Bottom water was collected at the same time at the same site by a Niskin bottle. Three cores were retrieved for incubation.

Sediment cores for methane concentration

The cores were plugged from top and bottom and incubated in a container filled with bottom water. A lens and a fiberoptic cable were attached outside of the core aiming at the Sensor Spot. A fibre-Optic Oxygen Meter Firesting O_2 sensor (PyroScience GmbH, Aachen, Germany), using the principle of dynamic luminescence quenching, was used to measure the oxygen concentration of the water. A one-point calibration of the sensors was performed, and the oxygen concentrations were logged continuously. The water was mixed and kept in motion by a magnetic stirrer, see figure 7. After a time, t_1, the top was removed and a syringe with a small hose was passed through the opening to sample the water. This was to minimise the amount of external water to mix with the samples. The water in the cores were then exchanged with fresh bottom water and the time reset. At a time, t_1+t_2, the water was sampled again. This was repeated to build up a time series t_1 + t_2 +…t_n. By gradually increasing the sampling intervals based on the simultaneous monitoring of decreasing oxygen concentrations appropriate time intervals for significant buildup in dissolved methane concentrations in the overlying water could be established.

The retrieved water samples were then stored, un-poisoned, at 2 °C awaiting analysis. Another sample retrieval method was tested where the cores were removed from the incubation tank, and the closing stopper was removed for sampling.

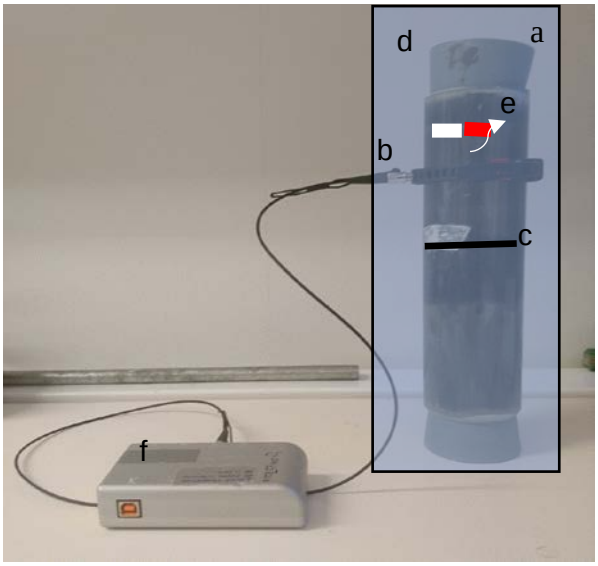

Figure 7: Schematic overview of core incubation. With: a) container with bottom water kept at 4 °C, b) fibreoptic cable attached to the outside of the contactless oxygen sensor, c) sediment surface, d) core plug, e) magnetic stirrer (external rotating magnet driving the rotation not shown), f) fiber-optic oxygen meter Firesting O_2.

. This method ensured no risk of mixing with the external water, however, both moving the cores and then refilling them with new bottom water greatly disturbed the sediments and this method was therefore not used further.

Lab analysis and postprocessing

Methane concentration

A headspace was created in the containers by the insertion of a needle through the septum. The needle was connected to a split valve helium source with the other connected directly, via a beaker of water, to the surrounding air. This ensured that there would be no creation of overpressure in the exetainers. A separate needle attached to a syringe was inserted through the septum into the container and an amount of water was removed. The water was thus replaced by helium creating a headspace. The exetainers were weighed before and after the creation of the headspaces and from the simple relationship

$$V_{headspace} = \frac{mass\ difference}{density\ of\ water}$$

The headspace volume was calculated. The amount of residual water (V_{water}) was calculated from

$$V_{water=}V_{tot-}V_{headspace}$$

Where V_{tot} is the volume of the container. The containers were then left to allow for the gas phase to equilibrate with the water over night. Since methane solubility in salt water is very low most migrated to the gas phase. The remainder was corrected for using the Bunsen solubility relationship. An aliquot of the headspace was then transferred to a syringe and analysed for methane concentration using a SRI 8610C gas chromatograph connected to a FID (Flame Ionization Detector) and an ECD (Electron Capture Detector). The mass spectrometer has a linked (series connected) double column injection loop of 1 ml each. The first column leads to the FID and the second to an ECD. A methaniser on the FID side reduces carbon dioxide to methane allowing it to be analysed during the same run. This dual inlet requires at least 2.2 ml of gas to be inserted to produce reliable reproducible results for *both* detectors.

The system is sensitive to water and an attempt to minimise water contamination by having an absorbent of sodium sulphate crystals enclosed within silicate wool inside the transfer syringe was tested. Samples run with this scheme exhibited a response that depended on the amount of gas, when the amount of gas was less than the 2 ml required to fill both columns, used and a strong drift in response during the day. Concurrently run standards returned a response within a 5% margin but the drift of the standard could be 20% by the end of the day. This was accounted for during postprocessing (of these small subset of runs) by assuming that the change in standard response could be approximated as a linear change. Subsequent testing found that the glass wool-Na_2SO_4 system released silica and salt dust to the injector. Testing without the salt-water removal system increased the water vapour contamination of the detector but removed the dependence of the amount of gas that was inserted as well as drift measured on the standard gas. All subsequent (May and onwards) runs were made without the water vapour removal system and exhibited no standard drift. For these measurements the standard response stayed within 3-5%.

A mixed standard consisting of 11.20 ±0.22 ppm CH_4,1.07 ±0.11 ppm N_2O and 1076 ±22 ppm CO_2 was used except for samples for the August 16 sediment core where a 11 ppt CH_4 was used.

The amount of methane in the headspace could then be calculated, using the general gas law, from

$$n = \frac{RT}{pV_{headspace}}$$

Where n is the molarity, R the gas constant, T the temperature in Kelvin, p the pressure, and V the volume. And the molarity, M, of the sample from

$$M = \frac{n}{V_{water}} = \frac{n}{V_{tot} - V_{headspace}}$$

This amount of dissolved methane was accounted for using Bunsen's solubility coefficient. Henry's law constant, H, can be defined as

$$H^{cp} = \frac{M_a}{p_a}$$

Where M_a is the molarity of species a and p_a is the partial pressure of species a in the gas phase. The Bunsen solubility, β, is defined by

$$H^{cp} = \frac{\beta}{RT^{STP}}$$

Where R is the gas constant (=8.314) and T^{STP} is the standard temperature (273.15 K). From these equations we can calculate the molarity of the remaining water as

$$M_{methane} = \frac{\beta p_{methane}}{RT^{STP}}$$

which then can be added as a correction factor to the molarity as measured and

calculated from the concentration of the gas phase. It has been shown by Weiss (1971) that the Bunsen solubility coefficient can expressed as a function depending on only the variables temperature and salinity. With the equation taking the form

$$\ln(\beta) = A_1 + A_2(^{100}/_{T}) + A_3 \ln(^{T}/_{100}) + S‰\left[B_1 + B_2(^{T}/_{100}) + B_3(^{T}/_{100^2})\right]$$

The constants have been determined experimentally and collated by Wiesenburg and Guinasso, 1979, based on experimental work by Yamamoto et al., 1976. With A_1 = -68.8862, A_2 = 101.4956, A_3 = 28.7314, S the salinity in per mill, B_1 = -0.076146, B_2 = 0.043970, and B_3 = -0.0068672. The correction, with the salinity and temperature in The Baltic Sea, generally works out to be an increase of about 2-3 %.

Alternative flux measurements

The methane concentrations measurements collected by the passive diffusion sampler, that measures across the sediment surface, was used to calculate the diffusive flux out of the sediments. From Fick's law of diffusion, we have:

$$J_z = D\frac{\partial c}{\partial z}$$

Where J_z is the flux in the z-direction, D is the diffusion coefficient, and ∂c/∂z is the concentration gradient across the sediment water interface. For our purposes D was assumed to be 0.87 x 10^{-5} cm^2/s.

Methane isotope analysis

Setup

All isotope analyses were performed using a Thermo Scientific Delta V plus™ IRMS (Isotope Ratio Mass Spectrometer) connected to gas chromatograph (GC) and, for low concentration samples, a GC IsoLink/PreCon system. Two methods were employed. For high concentration samples the sample was injected directly into the GC, oxidised to CO_2, and from the GC transferred to the Thermo Delta V IRMS. Samples with low concentrations had to be pre-processed with a PreCon system to enhance their concentrations prior to being transported into the GC. The concentrations of the sample headspace had been determined prior to this analysis by GC analysis with SRI 8610. Injection column size and standards were chosen accordingly. Too high concentrations would saturate the detector giving a false signal. Too low concentrations could be below detection limit or have their results skewed due to internal GC and/or PreCon fractionation effects.

Background

Since we cannot measure absolute quantities of an elemental species in a mass spectrometer, we instead compare mass ratios. The ratio R is defined as

$$R = \frac{abundance\ of\ heavy\ isotope}{abundance\ of\ light\ isotope}$$

These ratios are then compared to the ratio of a standard and referenced relative to a global standard expressed in the delta notation i.e. $\delta^{13}C\text{-}CH_4$ PDB (Pee Dee Belemnite). With the δ value defined as

$$\delta_{smp/std} = \left(\frac{R_{sample}}{R_{standard}} - 1\right)\ x\ 1000$$

with the international standard of PDB (Pee Dee Belemnite) and the unit given as per-mil. The conversion from our internal reference gas/standard is given by

$$\delta_{smp/pdb} = \delta_{ref/pdb} + \delta_{smp/ref} + \frac{\delta_{ref/pdb}\delta_{smp/ref}}{1000}$$

Which follows from the previous equation.

Sampling procedure

An aliquot of sample headspace was transferred to the injector port using an open syringe. High concentrations samples were injected directly into the GC (direct injection) using a glass syringe. Lower concentrations samples were pre-processed in a PreCon system were the

samples were purified (water removed in a water trap) and concentrated. In this case an aliquot of the sample was transferred from the vessel using a plastic syringe with an open tip. The way the samples were transferred could have a fractionating impact on the result, see discussion. And transferred through a septum to a column. The column could be exchanged, and 2 ml, 10 ml and 20 ml columns were employed The columns were chosen to conform to available amount of sample, concentration of said sample to stay within detector limits and to fit the chosen standard.

Prior to the start of all analyses a test on IRMS stability was performed. The linear response on the IRMS was tested by varying the amount of carrier gas so that the measured peak area varied from 1 to 6.4 V. The detector has a small linear drift with a slope of 0.016. Then 10 µl of a 100% CH_4 standard was analysed and compared to long term data. This was performed 4-5 times and the result was used as a reference for all samples and standards run that day. Then a new standard was run using a concentration and injection method comparable to the samples to be run. Any time the injection method or column size was changed new standards were run. Standards were also run half way through the run and as the last run to test the stability of the measurements. The long-term standard deviations of the standards were 0.272 for 100% CH_4 direct injection and 0.809 for 5 ppm CH_4 using the PreCon.

Postprocessing and peak area dependent fractionation

Measurements by Heike Siegmund and Joachim Jansen at Stockholm University have shown that this GC Isolink/PreCon system have a fractionating effect depending on the amount of sample used. Their tests were done by repeatedly analysing a standard but varying the amount used. Thus, they could link a fractionation effect relative to the peak area output of the IRMS (see Figure Appendix 1). An attempt to compensate by varying the amount of analyte used according to the known concentration was attempted, but the result was neither perfect nor possible for some samples since the operation was also constrained by the size of the available sample inlets, amount of available sample and the concentrations of available standards.

An attempt to compensate for this for samples with low available amounts of analyte was performed. Figure Appendix 1a show a strong linear dependency, with a R^2 of 0.9663, for low concentration measurements using direct injection. The same is true for the PreCon but here the standard deviation of each measurement is higher, and the scatter is much stronger. For the analysis with direct injection we adjusted our data according to the regression curve from Figure Appendix 1a. However, this was not attempted for the PreCon-data since the deviation given by the regression line was within long term standard deviation.

For direct injection of low concentrations, we have:

$y = 0.3461x - 39.633$ $R^2 = 0.9663$
and
$y = 0.0158x - 37.642$, $R^2 = 0.5972$.

For peak areas below and above 7.1 V, respectively.

The ideal area is 7.1 V for direct injection. By comparing the deviation in areas, which were lower than 7.1 V, to that of the 7.1 V reference, results were adjusted accordingly, i.e.

$$adjustment = (7.1 - area\ output)\ x\ slope$$

We assume that there is no fractionation due to the gas-water phase equilibria based on work by Know et al. (1992), who found that dissolved CH_4 in the surface water in equilibrium with the atmosphere provides similar values as CH_4 in the gas phase

Alkalinity

The alkalinity of the water samples was determined using a Methrohm Titrando™.

The samples were diluted by factor 2.7 for 12 ml exetainers samples and 10 for 6 ml exetainer samples. Although the pH electrode used was past the recommended expiry date, the pH calibrations performed before the start of each run was less than 0.03 units and was deemed suitable for our purposes. The alkalinity was calculated from the added acid-pH response by titration to pH 4.5 and assuming that the contribution from the milli-Q® dilutant was negligible.

Results

Water Column CTD

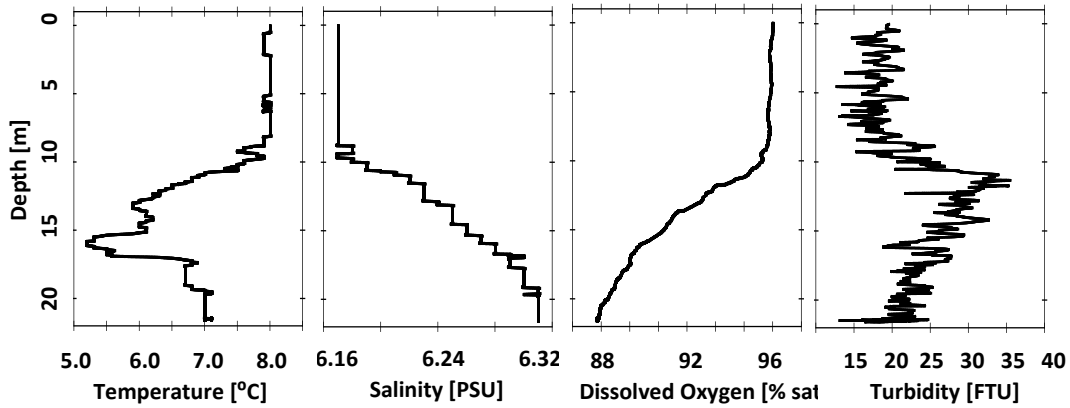

Figure 8: Temperature, salinity , dissolved oxygen and turbidity for the water column mid-November.

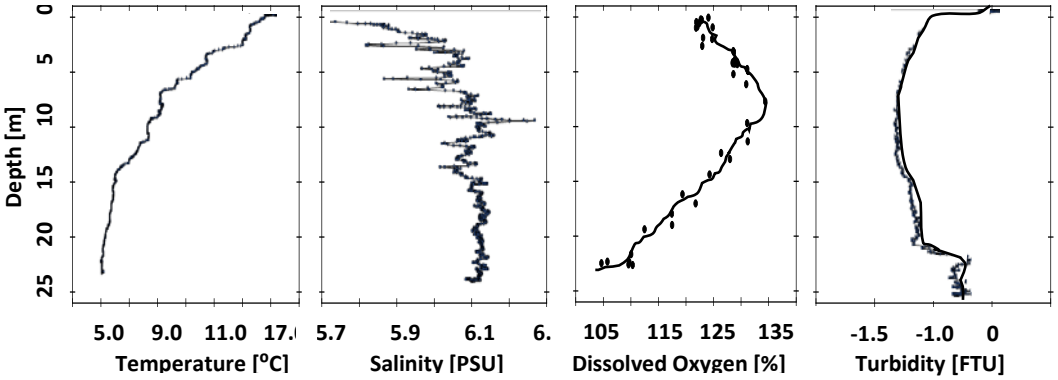

Figure 9: Temperature, salinity , dissolved oxygen and turbidity for the water column May.

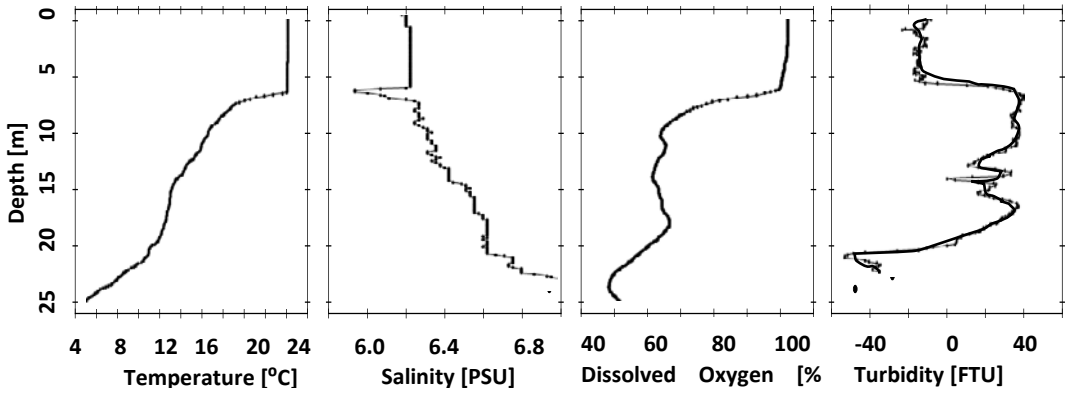

Figure 10: Temperature, salinity , dissolved oxygen and turbidity for the water column August 6th.

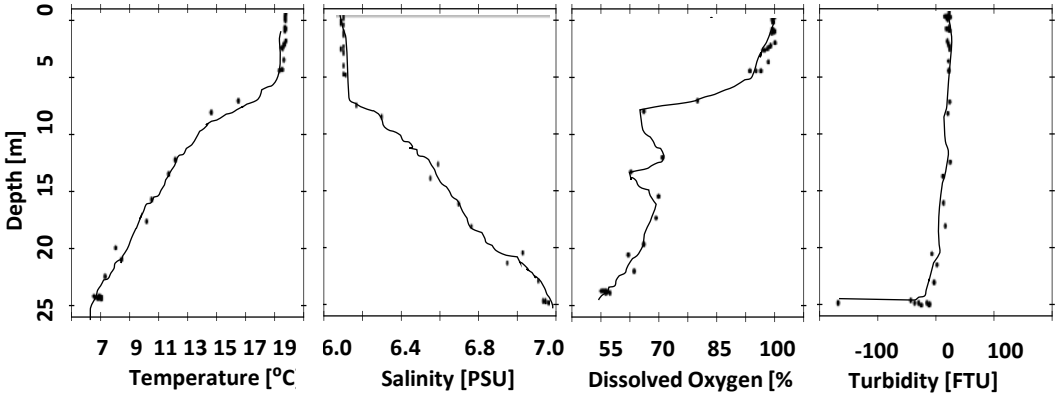

Figure 11: Temperature, salinity , dissolved oxygen and turbidity for the water column August 16th.

Water Column

Figure 8 through 11 shows the physical properties of main interest for the water-column sampled during a day in November and May and during two days in August. All collected at the same site around noon. In November the water column is very well mixed for the top ten meters followed by a thermocline with a decrease in temperature of 3 °C in five meters. Whereupon the temperature increases again with 2 °C in 3 meters further down, followed by a stable well mixed layer for the last two meters above the sediments. The change in salinity and dissolved oxygen initially follows the temperature with both a halocline and oxycline at 10 meters depth. At this depth there is also a maximum for the turbidity. Past the 10 meters mark oxygen decreases whereas salinity increases both without any great gradient changes. The water is well oxygenated throughout the water column from 100% at the surface down to 88% at the benthic boundary layer.

By mid-May the strong -clines have disappeared with temperature going from 17 °C at the surface to 5 °C at the benthic boundary layer without any sudden changes. Oxygen[6] starts high with a 25 percentage over saturation increasing to a maximum at 8 meters depth and then decreasing down to 105% saturation at the benthic boundary layer. Turbidity is high at the surface but low throughout the rest of the water column.

By August a strong thermocline has developed at 5 meters depth. Mirrored by a halocline at the same depth. The water is oxygen saturated for the top 5 meters decreasing to 60% in 5 meters. In August 6th, compared to 16th, there is also a change in water composition at 20 meters depth. The temperature and salinity gradients changes as oxygen decreases and the absolute value of the turbidity increases.

The Benthic Boundary Layer

These same water properties were also gathered for hours or days after the water column data was collected. The data was gathered through by the same CTD, with the same calibrations, as the water column was. The data was gathered through the movement of a lift on a benthic lander to which the CTD was attached. The lift performed repeating cycles so the depth the CTD was collecting data from was the same depths throughout each deployment. The measured pressure has been used as a proxy for depth and the depth variations are thus not true depth changes but rather changes in measured pressure. Figure 12-14 shows the water properties of the water column in May and August. One of the cycles for each date is highlighted in blue for all the water properties. Each cycle was approximately 4 hours.

The highlighted blue cycle (figure 12) shows how the lift pauses at different depths to collect data. However, during this cycle there is no real trend with depth for neither temperature, salinity turbidity, photosynthetically active radiation, nor dissolved oxygen. There are abrupt changes in all measured parameters the but not tied to the position of the lift and thus not tied to a change with depth. At the end of this data set there is a decrease in water temperature of 2 °C in less than two hours. It is coupled with an increase in turbidity and salinity and a decrease in dissolved oxygen. It can also be seen that the photosynthetically active radiation reaches 1.2 micro Einsteins at the commencement of the measurement.

At August 6th, for which there is a larger data set, there is some cyclicity in the temperature data coincident with the depth where the data was collected. With changes of approximately 1 °C over a 60 cm interval in the benthic boundary layer. The rising and setting of the sun can clearly be seen from the PAR data which now peaks at 0.5 micro Einsteins. The dissolved oxygen decreases swiftly approaching the sediments from an almost 60% saturation 60 cm above the sediment-water interface down to 0% dissolved oxygen just above the sediment surface.

The oxygen follows the same trend for the August 16th deployment for the first two cycles after which any strong correlation with depth disappears. We can also see that the water temperature in the benthic boundary layer increases with nearly 2.5 °C during cycle 11. From the PAR measurements a significant decrease in incoming solar radiation during day 3 can be deduced (with its maximum during cycle 16 during which a substantial change in the turbidity also takes place.

[6] It is possible that the oxygen sensor was not correctly calibrated for this measurement. The absolute values would then be off, but the trends represented correctly.

Benthic CTD data

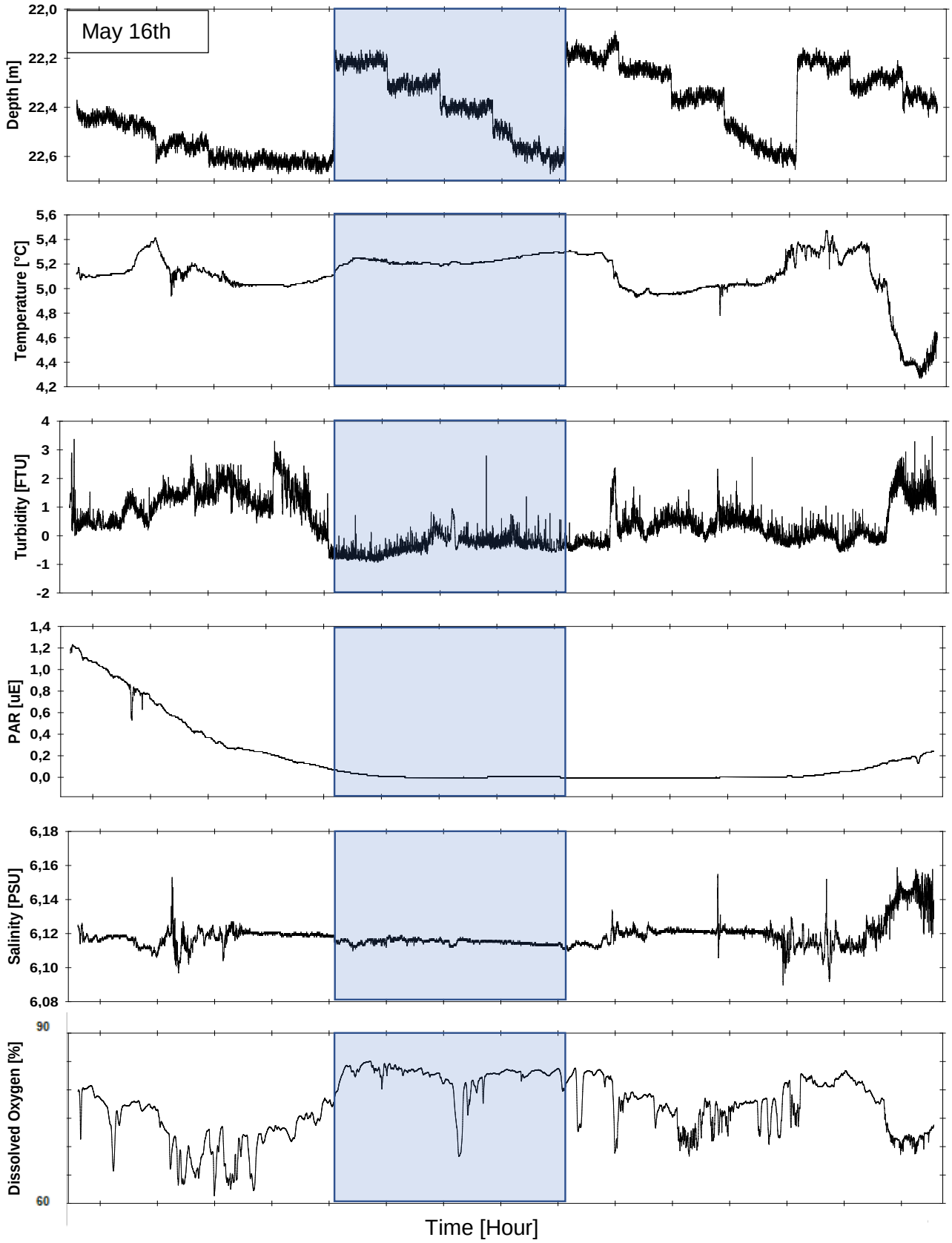

Figure 12: Benthic CTD data during three lift cycles. Each cycle, one of which is highlighted, is approximately 4 hours. One lift cycle has been highlighted in blue.

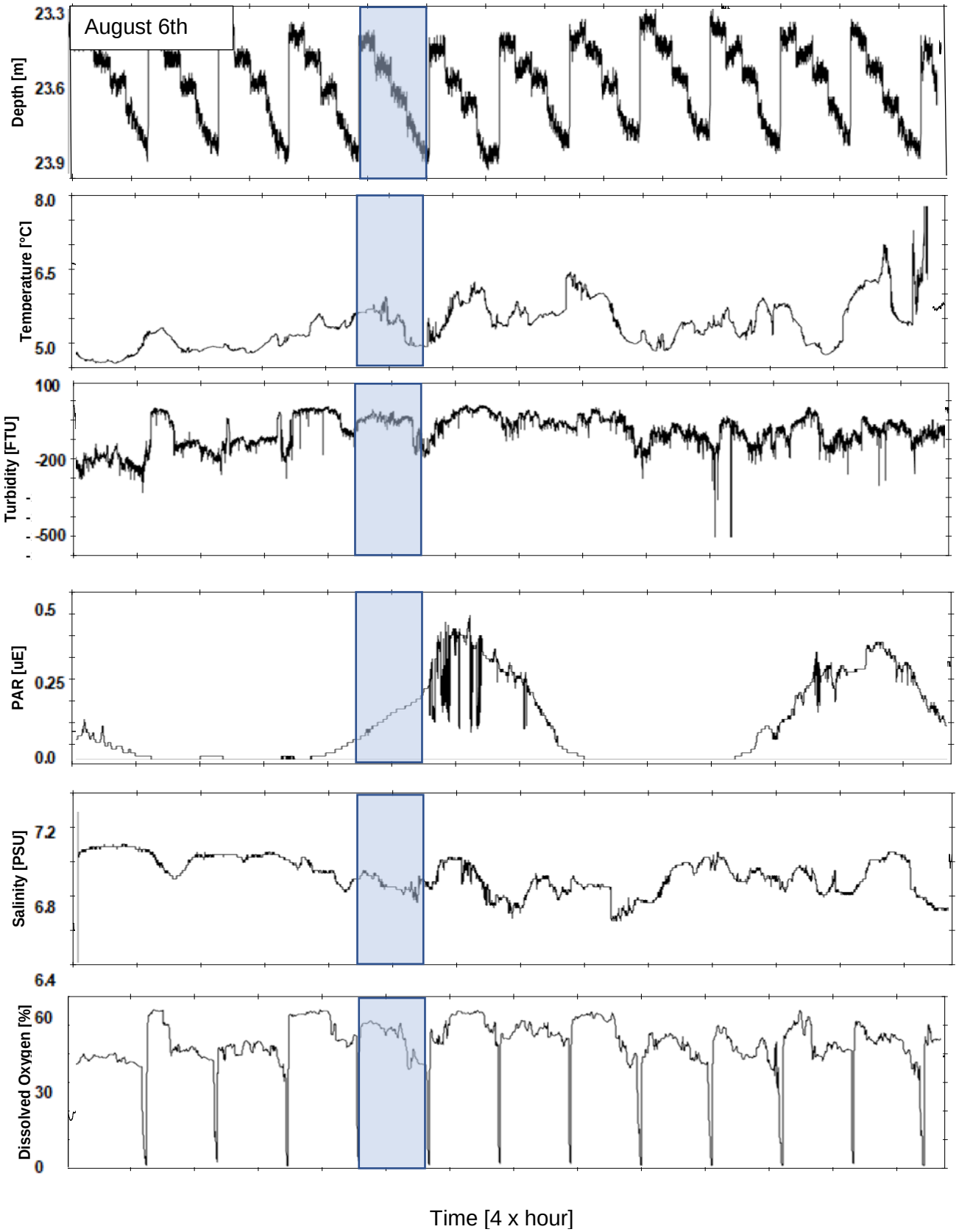

Figure 13: Water properties collected by a lift-mounted CTD attached to a benthic lander. The stepwise patterns in the first graph is due to the lift movement of the CTD. The pressure measured by the CTD have been used as a proxy for depth. One lift cycle is approximately 4 hours. The total movement of the lift is 60 cm. One lift cycle has been highlighted in blue.

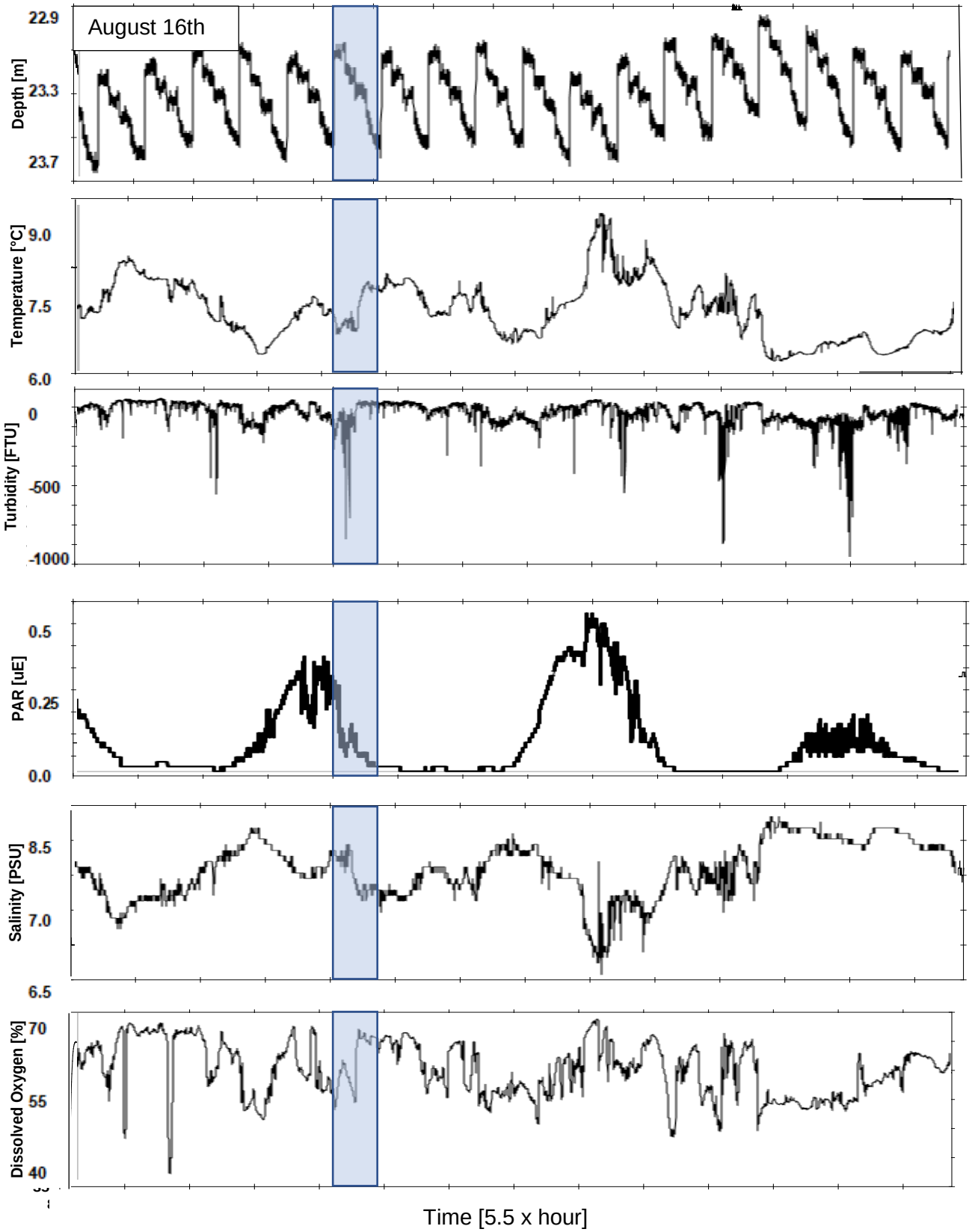

Figure 14: Water properties collected by a lift-mounted CTD attached to a benthic lander. The stepwise patterns in the first graph is due to the lift movement of the CTD. The pressure measured by the CTD have been used as a proxy for depth. One lift cycle is approximately 4 hours. The total movement of the lift is 60 cm. A lift cycle has been highlighted in blue.

Benthic boundary Layer Current Velocity Profiles May 16th

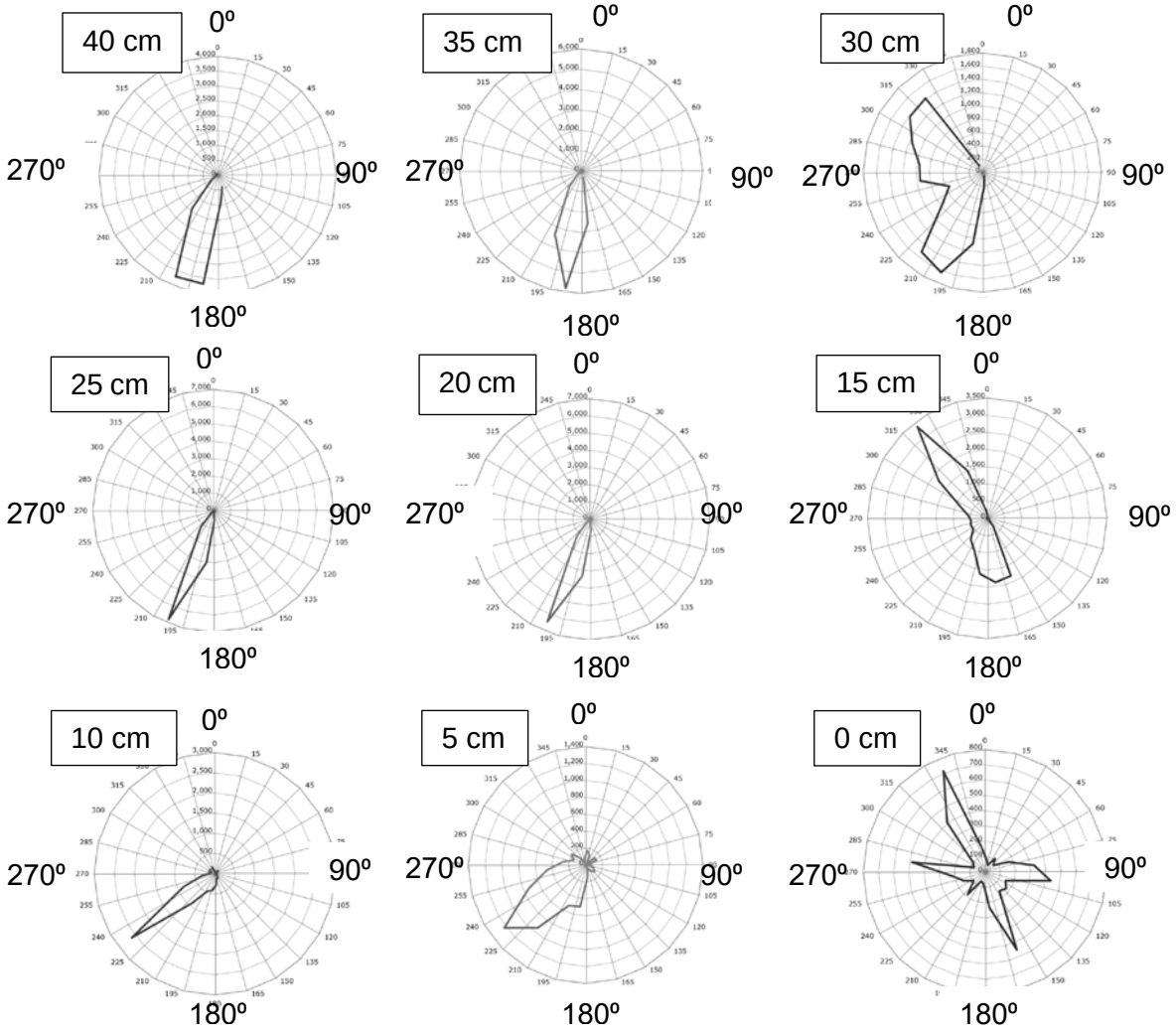

Figure 15: Current roses for May 16, averaged between 16:00 and 16:08, by their distance above the seafloor.

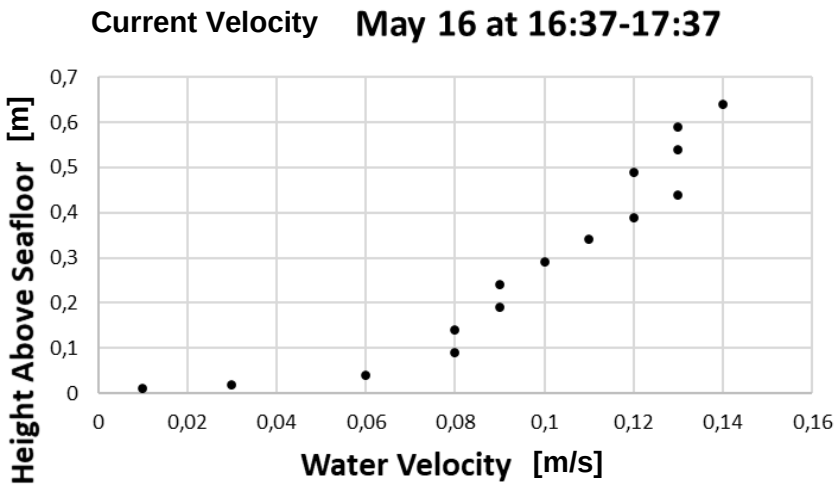

Figure 15: Average current velocity profile for the benthic boundary layer.

Comparing two velocity profiles, one from May and one from August (figure 15 and 17), it is noticeable that a current velocity of 14 cm/s at 65 cm above the seafloor is strong enough for the current to exhibit a gradient for the full range the ADCP can measure. Not reaching a stable free flow velocity at this distance from the seafloor. The free flow velocity is 9 cm/s for both examples shown in figure 17, however, their gradients differ close to the seafloor for these two cases.

Benthic boundary Layer Current Velocity Profiles August 6th

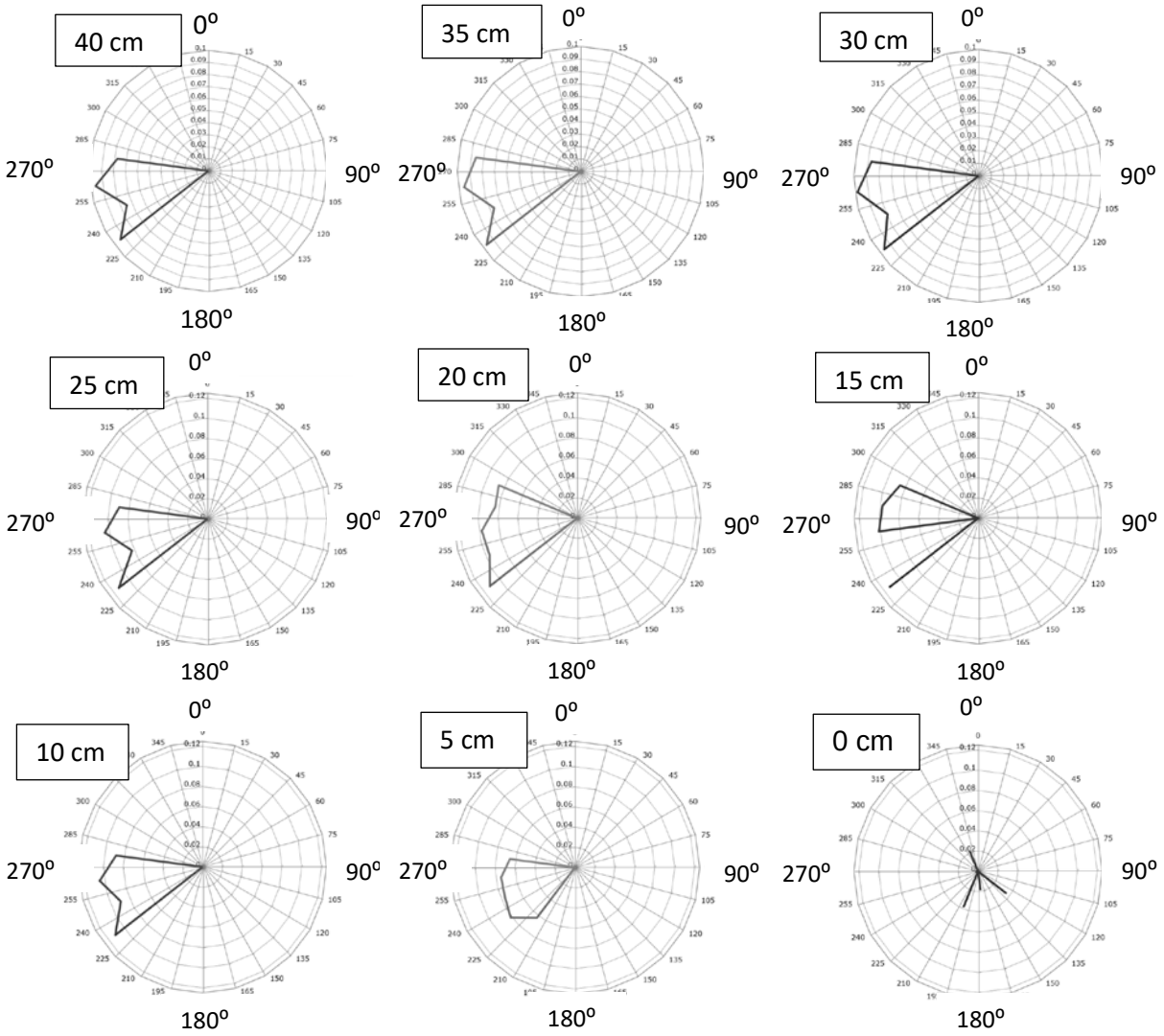

Figure 16: Current roses for August 6th, averaged between 16:00 and 16:11, by their distance above the seafloor.

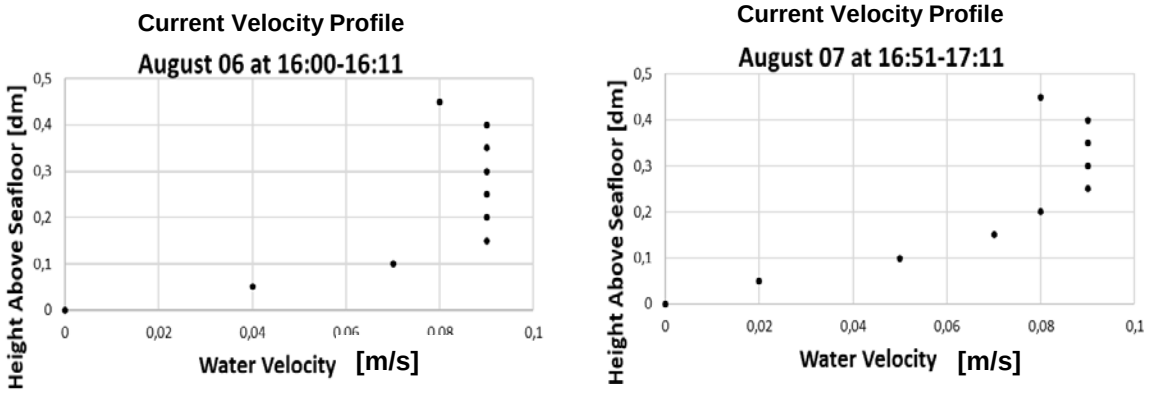

Figure 17: Average current velocity profile for the benthic boundary layer averaged over 10 and 20 minutes respectively during the afternoons of August 6 and 7.

The standard deviation of all current velocities is 0.03 m/s. The current roses show the direction of the current for the water layers for these 10-60 minutes. The direction changes with depth but not enough to show a strong Ekman layering. The may direction profiles exhibit two current directions for the layers at 15 and 30 cm above the seafloor. Not seen in any other layer. Note the reduced velocity at 0.5 m above the sediment surface that is evident in all three graphs in figure 15 and 17.

Benthic Boundary Layer Water Properties Time Series

As we can see in figure 18 and 19 there are both variability in speed (3-70 cm/s) and direction (direction in blue in figure 18) of the currents. Except for some anomalies the temperature is close to 6 ºC throughout the deployments. However, there is an instant when the temperature increases with 5 °C and the current velocity increases by approximately 300% in less than half an hour (section marked in peach).

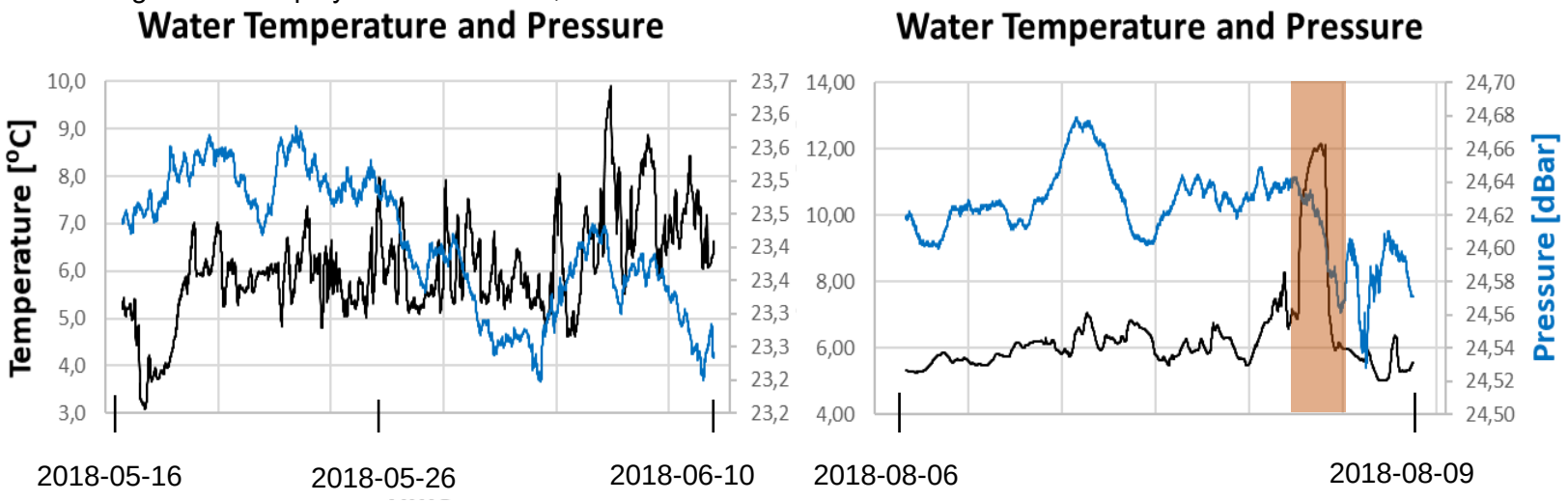

Figure 18: Temperature and pressure time series as measured by the ADCP. The instrument was situated 74 cm above the seafloor during the May deployment and 64 cm above the seafloor during the August deployment. A temperature anomaly for the August deployment is highlighted in peach.

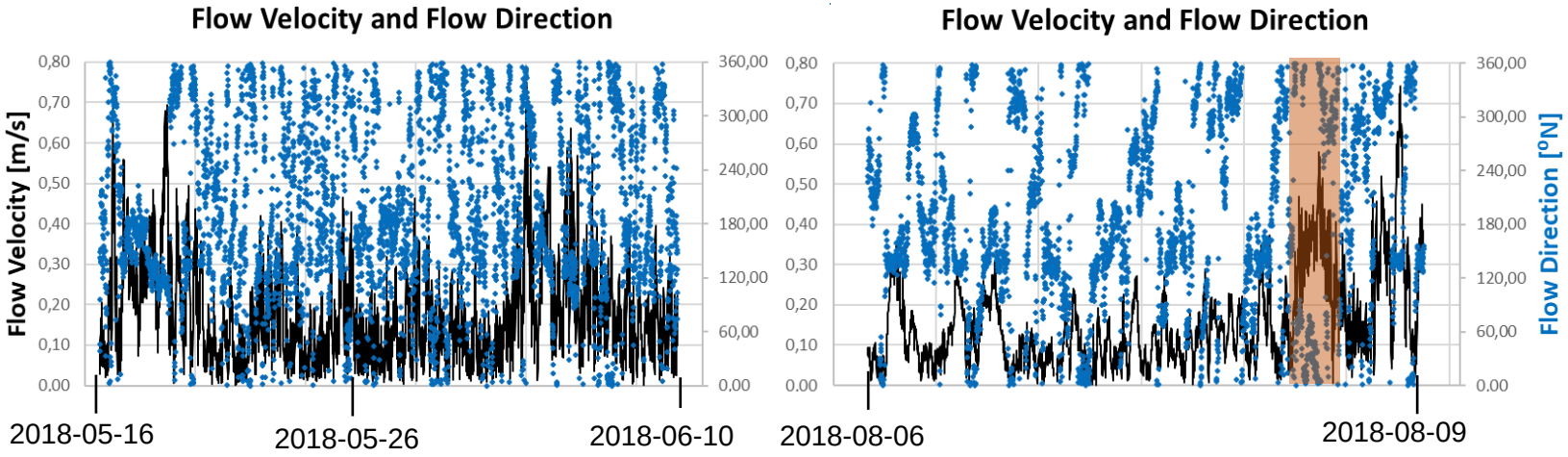

Figure 19: Flow velocity and direction time series for two deployments. The parameters are 15 cm below the sensor head.

Temperature and Velocity Anomaly

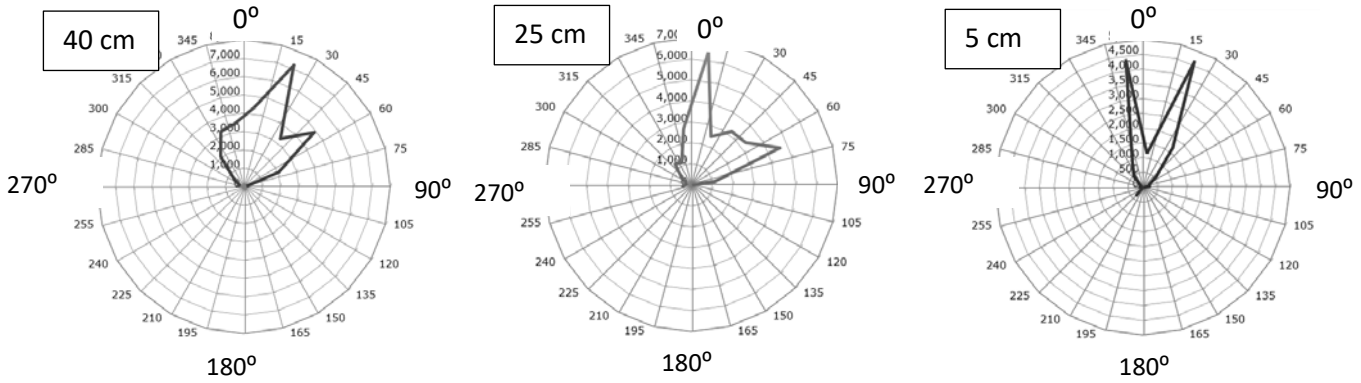

Figure 20: Current rose showing speed and direction of the currents for the 4 hours of the temperature anomaly at 3 heights above the seafloor.

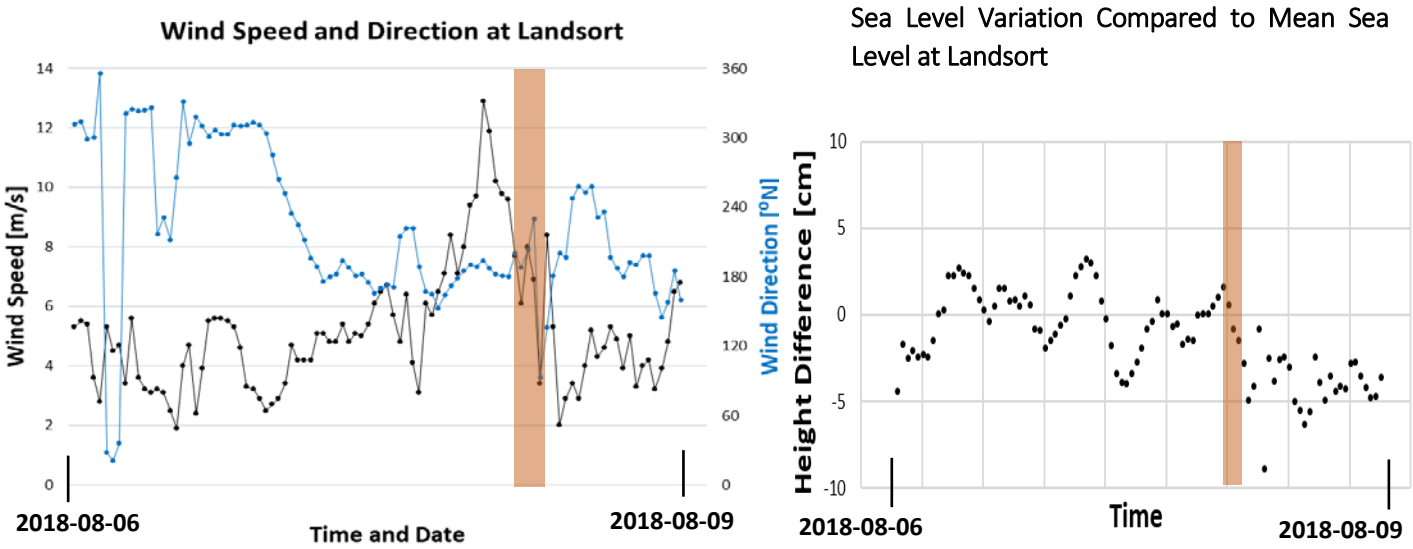

Figure 21: Wind speed, wind direction, and sea level variation measured at Landsort, 13 km to the south east of the lander position. The section marked in peach is the time of the bottom water anomaly.

From figure 21 it is evident that there is an increase in wind velocity from an ambient 6 m/s to 13 m/s hours before the bottom water temperature anomaly. We can also see that the wind is generally southerly or northerly during these three days. The sea level starts do decrease at the onset of the anomaly at Landsort. Decreasing by 5 cm before stabilizing (figure 21, right). The current direction (figure 20) is north to north-east during the anomaly with two distinct directions. The current directions changes with distance above the sediments.

Methane Concentration

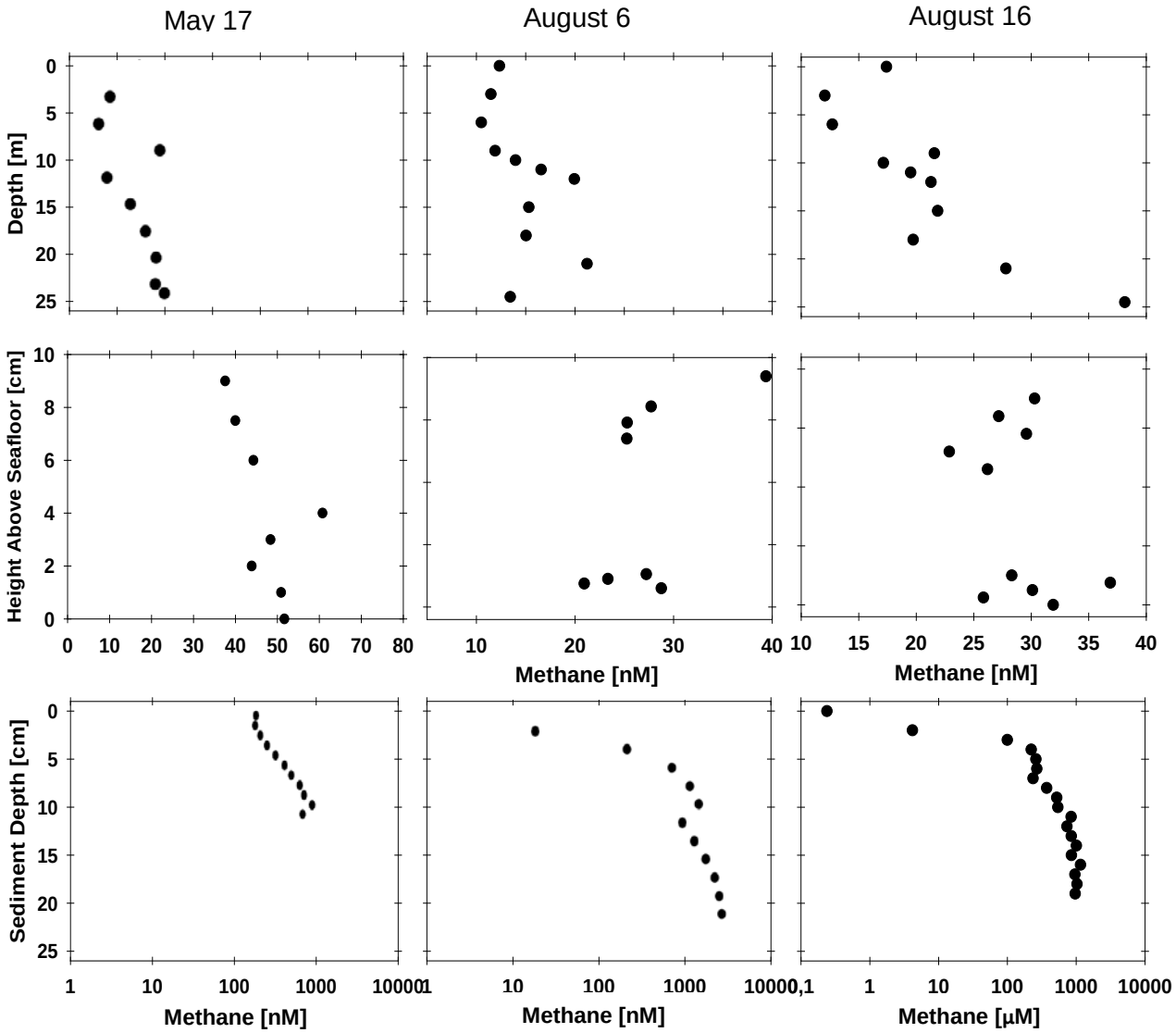

Figure 22: Methane concentration in the water column, BBL, and sediments May 17th. The concentration in the sediments have not been corrected for porosity but are rather moles per litre sediments. Please not the change in scale in going from water to sediments and that the sediment samples from August 16th are in µM whereas all other are in nM.

The dissolved methane concentration in the water column, benthic boundary layer and sediments for three sampling times are shown in figure 22. The concentrations as well as their maxima and minima varied between samplings. Despite the fact that an attempt was made to perform all sampling at the same location the methane concentration in the porewater was nearly a factor 100 higher at August 16 compared to August 6. The methane concentration just below the water-sediment interface was 16 nM august 6 compared to 173 in May and 237 nM on August 16. The concentration in the benthic boundary layer varies between sampling dates. With a 51.7 nM concentration in May at the sediment-water interface, compared to 25-30 in August. In May there is a strong concentration gradient in the benthic boundary layer and at 9 cm above the sediments the methane concentration has decreased to 38 nM. The water column methane concentration at the surface are at all sampling times supersaturated relative to atmospheric concentrations and exhibits maxima in the water column at 9 (May), 12 and 22 (August 6), and 9 and 12 (August 16). metres depth respectively. With a standard deviation, as measured on the standards, of all water column samples of 5-10%. The error in sediment depth are estimated to be ±1 cm.

$\delta^{13}C\text{-}CH_4$

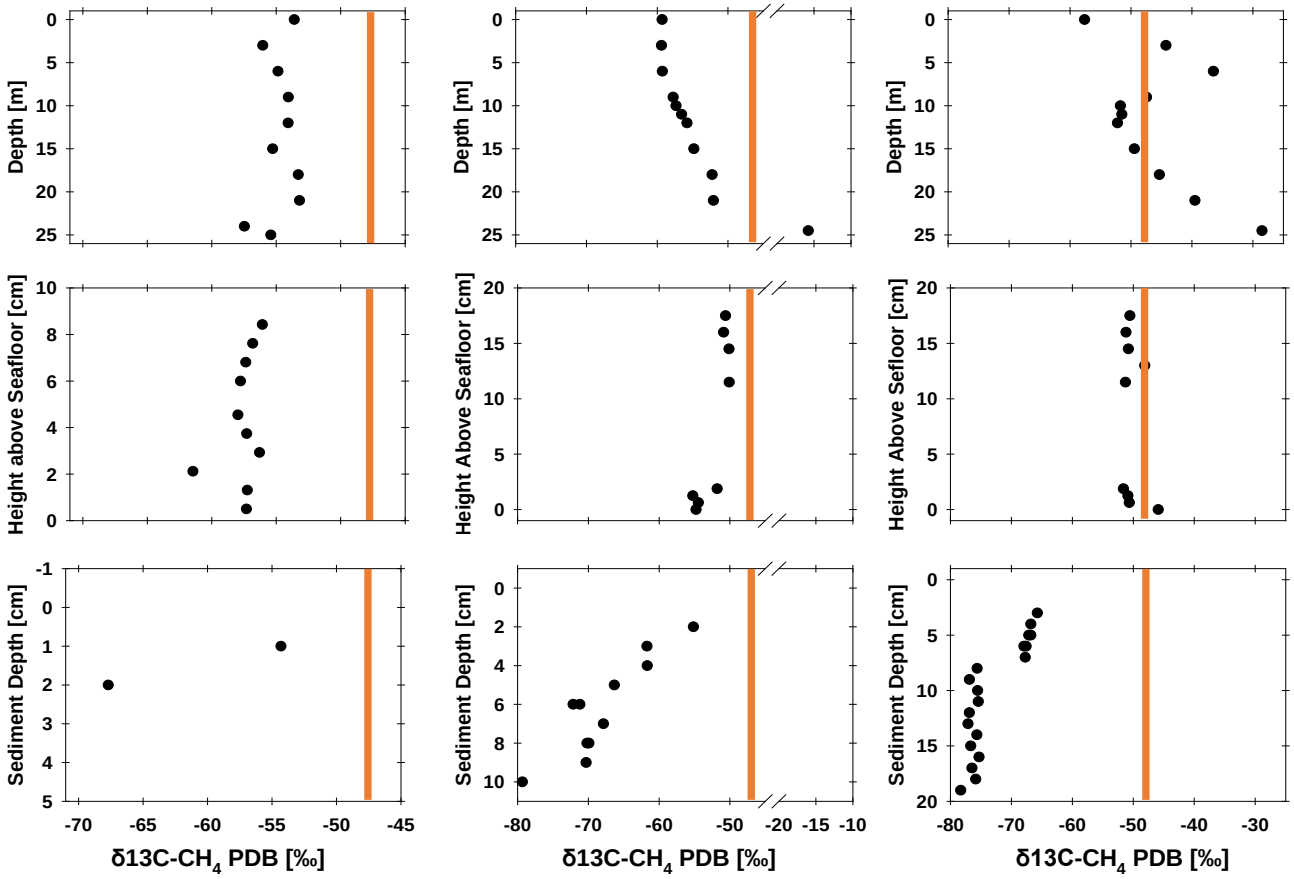

Figure 23: δ13C-CH4 of dissolved methane in the water column, the benthic boundary layer and the sediments collected at three times from the same site. The orange line indicates the value of average atmospheric equilibrium of -47.5‰(Morimoto et al., 2017). Please not the different scales that have been used for the three columns.

The $\delta^{13}C\text{-}CH_4$ results from the three sampling times are collected in figure 23. In the sediments the lowest values are at depth with values close to -80‰. A shift to heavier, -68- -70‰, occurs over just a centimetre distance in both August cores at 8-10 centimetres depth. At the sediment surface the isotope composition is between -58 and -52‰ with a slight trend toward the positive over the first 20 centimetres into the benthic boundary layer. In the water column the isotope trend is distinctly different at different sampling times. The May data shows two strong negative excursions, at 3- and 15- meters depth respectively. Changing by more than 3‰ compared to the directly over and underlying pore waters. No such minima are evident for the water column at August 6 which, however, has a -15‰ outlier at 25 metres depth. The August 16 water column has two minima. One at 11 metres depth and one in the surface water. The surface water is not in isotopic equilibrium with the atmosphere (line in peach) but rather lighter at all times. The standard deviation for the water column is 0.272‰ and 0.8‰ for the sediments (except the top 5 centimetres which are also 0.272‰).

Comparing alkalinity and dissolved methane for DET and and normal water sampling

Water Samples *Hesslein Sampler*

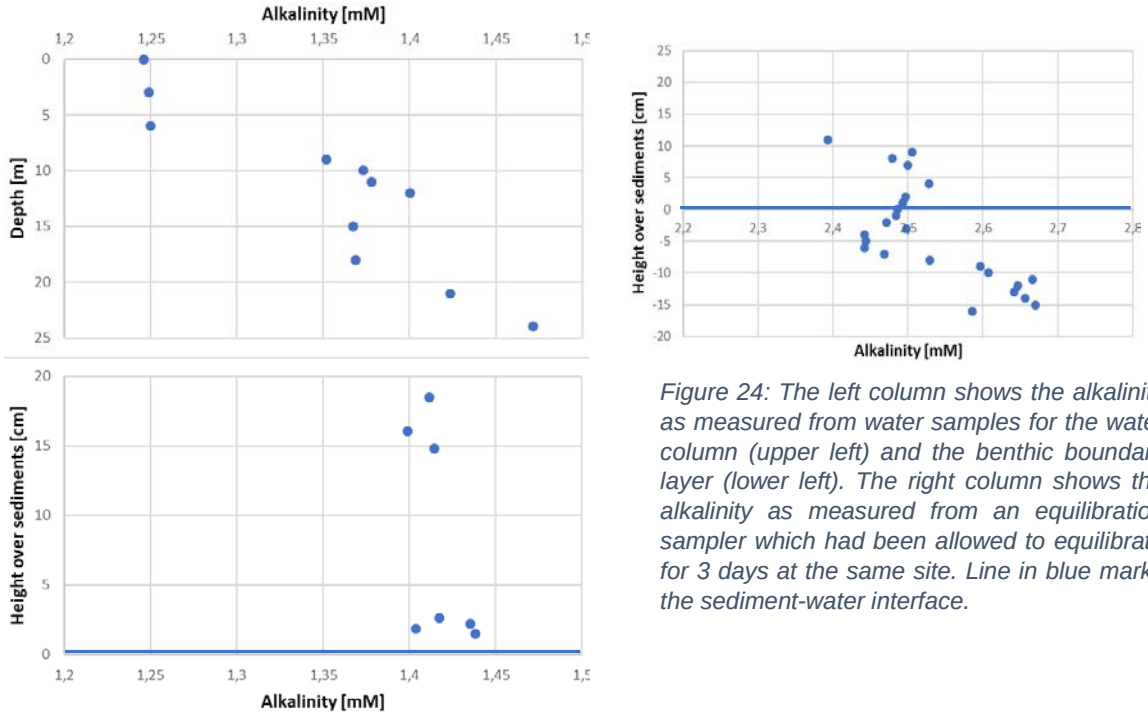

Figure 24: The left column shows the alkalinity as measured from water samples for the water column (upper left) and the benthic boundary layer (lower left). The right column shows the alkalinity as measured from an equilibration sampler which had been allowed to equilibrate for 3 days at the same site. Line in blue marks the sediment-water interface.

Sediments from core Hesslein Sampler

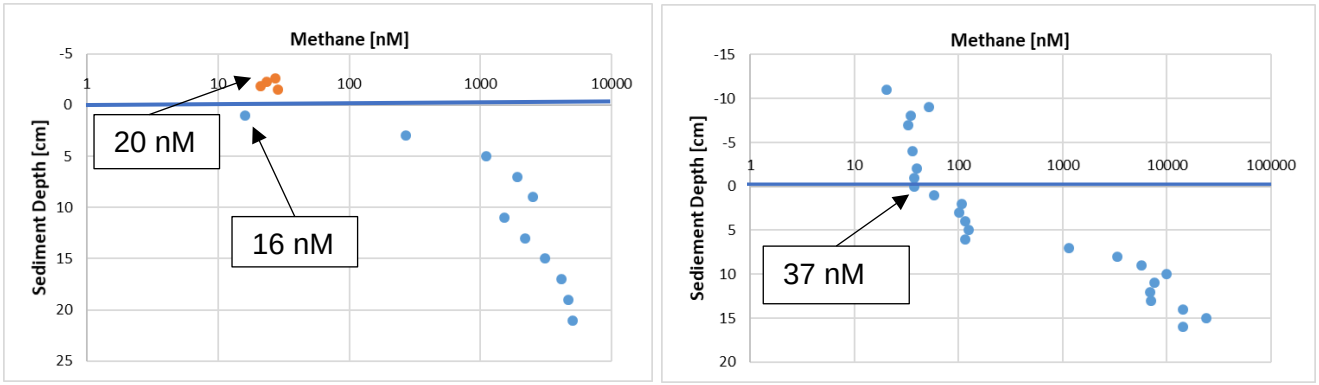

Figure 25: The column of the left shows alkalinity and methane concentrations collected via water sampling and by retrieving samples from a sediment core August 06. The column of the right shows the data from the Hesslein sampler that was inserted at the same time and left to equilibrate for 3 days. The porewater methane (left) have not been corrected for porosity but rather shows the sediment concentration. Blue line marks the sediment-water interface.

Figure 19 shows the alkalinity for the water column and the benthic boundary layer as measured on collected water samples (upper left column) and for the benthic boundary layer and the upper 10 cm of the sediments collected by the DET sampler (upper right). The alkalinity of the water column starts at 1.25 and increases to 1.35 at the thermocline. At 15 m it decreases again after which it increases down to the sea floor. In the BBL there is a small increasing trend towards the sea floor but with a large DET samples also exhibit a spread but exhibits more than a mM higher values at the sediment surface. When it comes to dissolved methane the discrepancy between water samples and DET samples are similar. Water samples and sediment samples give a value for dissolved methane of 16-20 nM whereas the result from the Hesslein sampler gives 37 nM at the sediment surface.

Discussion

BBL water data

From the Benthic CTD data we can see how small the water property changes are over the small depths that the CTD was moved, excluding oxygen concentrations. The largest changes occur when new water masses move into the area with their own intrinsic properties. From the benthic CTD data (most evident in the August measurements, figure 13-14) a pressure change is evident Since there is no indication of diurnal tides this change is most likely related to higher water that has built up as an effect of winds or high-low pressure areas and that this forces a large movement, and thus exchange, of the water mass. This returns to the problem of how representative a single measurement of the water mass is and how they can be used to scale up. There is also a problem for data collected using a benthic lander system. Since the changes in water properties are due to exchange of water which in turn is a result of atmospheric conditions, high/low pressure regions, it is always a risk, no matter how sensibly the lander is placed, that one or several sensors, at one or more times, are positioned so that the measured properties are influenced by self-induced turbulence from the lander itself. However, the current velocity data can be used to create a progressive vector path (figure 25) for the ter moving past the detector. In the area of interest, it is clear that there are two main current directions: one northwest to southeast and one southeast to northwest with the total transport being dominantly southeast. The two opposite-direction transport slows the effective transport of water out of and into the area. The water effectively "sloshes" around. The one main deviation from this observation occurred August 18 when elevated temperature (+5 °C) bottom water was recorded, in conjunction with a dramatic (+300%) increase in current velocity, and 90° change in current direction (see progressive vector path marked in peach in figure 25). This was observed following hours of very high (14m/s) winds recorded south of the area. This deviation, in water properties and current velocity, is most easily explained by downwelling due to wind induced water movement. This fits well with observations made by marine biologist working in the area who frequently find evidence of upwelling when working in the waters around the nearby Askö island (Lena Kautsky, personal communication).

On the trustworthiness of Method

Current behaviour in the benthic boundary layer

From the evidence given by the varying current velocity gradients arising from the same free flow velocity (figure 17) it is evident that the reality is more complex that the behaviour expected of near boundary flow derived from the Navier-Stokes equation. hat a purely, so called,

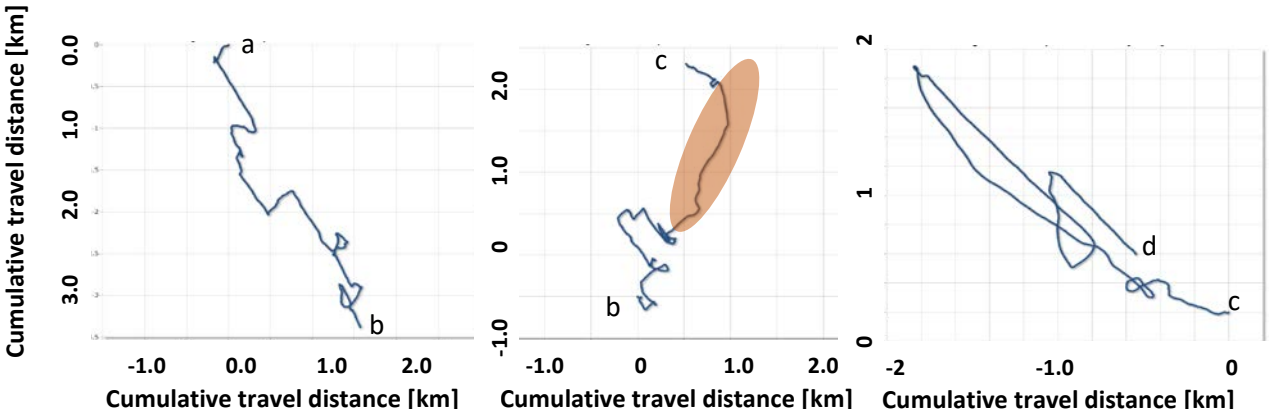

*Figure 25: Progressive vector path showing how a particle at starting at **a** would travel through **b** and **c**, ending up at **d**. In time a-b represents 16:01-20:25, b-c represent 20:27-00:51, and c-d represents 00:54-09:00. Starting at August 06 and ending august 08.*

logarithmic law of the wall-argument to derive the behaviour of the currents near (0 - 25 cm) the sediment-water interface does not actually hold. And that theoretical arguments on how concentrations of solutes should be given predicted, likely false, velocity gradient is at best naïve. The fact that the velocity changes rapidly and rarely, if ever, is constant also nullifies and rejects any arguments simply based on measurements in one location at one time. In fact, measurements over long time is vital for any reliable predictions or attempts at extrapolation. It can be speculated that the reason for this departure in what we see from what the theory predicts can be explained by several assumptions and observations.

1) The Navier-Stokes equation assumes an infinite, perfectly fat well-defined boundary with a no slip condition at the boundary surface.,

Not only is the sediment surface not infinite nor perfectly flat it is also poorly defined and, in a sense, not even a proper surface. The soft topmost sediments are very easily disturbed and when the current velocity can range between 5 and 75 cm/s in a single day (figure 19) it is not unreasonable to assume that both accumulation and suspension of sediments can occur.

2) It has been shown (Holtappels 2011) that the log law of the wall doesn't properly predict behaviour when the water is gravitationally unstable (vertical movement).

We have seen several instances of downwelling with warm, less saline water. This water would be gravitationally unstable, and these are also instances where the log wall of the wall would not hold.

So, in conclusion, no reliable conclusions can be drawn from point measurements and extrapolations. Rather, long term high resolution measurements are needed to make predictions of solute behaviour in this highly dynamic setting. Current data should always be collected when samples from the BBL are retrieved.

Passive DET-samplers vs water sampling

From the measurements on alkalinity and methane concentration in the transition from sediments to water it is clear that the passive sample chambers pervadingly contain water with both a higher alkalinity and a higher amount of dissolved methane relative to that of water retrieved with the peristaltic pump. The water samples retrieved with the peristaltic pump agree well with the concentrations in the sediment-water interface sampled from sediment cores whereas the Hesslein sampler yet again yield more than double that concentration (see figure 25). Given how the Hesslein sample is employed I find it likely that it overestimates all concentrations. The Hesslein sampler was attached to the lower end of the lift part of the benthic lander. The benthic lander itself is nearly 2 meters high and despite its mostly hollow structure the drag imposed on it by the moving water is non-negligible. In addition, the structure is somewhat rickety. I find it likely that the changing current will cause the structure to move slightly, transferring some of that movement to the Hesslein sampler enough to disturbing the sediments and disturb the sediments enough to open a pathway for enhanced solute transport at the point of insertion.

Methane

Local or transported

From the isotope data it is clear from the signature that that the dissolved methane in the water column is not, isotopically, in equilibrium with the atmosphere. It is in fact always lighter. For the August measure-ments it is also lighter than the methane released from the sediments as exhibited by the samples from the benthic boundary layer. There are three simple explanations for this discrepancy: 1) The low $\delta^{13}C$ values in the upper regions of the water columns are due to light methane released as bubbles carrying the low $\delta^{13}C$ signature up

through the water column to the upper layers. 2) Produced in situ. 3) Not related to the methane released from the sediments here but rather due to lateral transport and produced elsewhere. Possibly even groundwater from the shore.

Lateral transport can be dismissed even though we know that the water is not stationary it still fails to explain the low $\delta^{13}C$ values. If it was transported from elsewhere then the problem is only moved not solved because then we need to find an explanation for why that region exhibits such low $\delta^{13}C$ values. Also, the hypothesis that the surface water carries a groundwater-soil signal can be rejected on the grounds of weather. The weather during the sampling period was hotter and drier than usual with very low groundwater levels. The situation would more likely lead to seawater infiltration of the groundwater reservoirs rather than expulsions of groundwater lying like a lid on top of the seawater several kilometres from land.

Ebullitions

An attempt to measure the effect of ebullition was made using a benthic bubble trap. It was only deployed twice. The first time it was deployed for a couple of hours several millilitres of gas was found in the trap. The trapped gases had a methane concentration several times higher than the ambiance atmospheric level (11.25 ppm). That so much gas was trapped in such a limited amount of time can be explained by expulsions due to sediment disturbance when the lander was deployed, and gas already trapped in the bubble trap as it was deployed. We cannot exclude the possibility that some, or even most, of that gas wasn't surface-air trapped in the bubble trap as it was deployed. However, the fact that the methane levels were higher than atmospheric indicates that at least some of the trapped gas had an ebullitive sediment source. The second time the bubble trap was deployed for ten days and no hint of ebullitions were found. This would indicate that there are no continuous ebullitions coming from the sediments we cannot disregard the possibility of transient or localised expulsions as seen by Jakobsson et al., 2016. It is also highly unlikely that the methane maxima in the water column are related to exchange with bubbles passing through. With a bubble velocity of 10 cm/s or higher (Talaia, 2007) and low solubility a substantial portion would not have time to diffuse into the water column. And, either way, would not be able to explain the localised maxima.

Two upper water column sources?

In addition, both times (May 16, August 16) when the water column exhibits some stratification there are two distinct layers of highly depleted $\delta^{13}C\text{-}CH_4$. One associated with the pycnocline and the other at shallow, ~3 m, depth. The pycnocline is a zone that attracts animals of all kinds due to the ample supply of food and it can therefore be presumed that methane is being produced there in anoxic micro-environments, e.g. the guts of grazing copepods (Schmale et al., 2017. These dual depletion layers could feasibly be explained in two ways, or a combination of two. Either we have 1. Diel migrations of grazers (zooplankton) moving between the surface area and the pycnocline (Lampert, 2003). This would enable them to feed on phytoplankton at the surface and dead organic particulates accumulating at the pycnocline while avoiding predators (e.g. see discussion by Hayes, 2003). Or, 2. we have an alternative source of methane in the photic zone directly through different means, possibly tied to nitrogen fixation as shown by Zheng et al., 2018. Or, 3. a combination of 1 and 2 taking place at the uppermost water layer.

A strong thermogenic source?

The local atmospheric background of 1.86 ppm with an isotopic composition of -47.5‰ (Morimoto, 2017) can be assumed to be a mix of "normal" atmospheric background (-47.3‰), diffusion from the supersaturated surface water (-60‰) and ebullitions of a thermogenic source (-40‰, Söderberg and Laier, unpublished). From a simple isotopic

mass balance argument, it is obvious that the major component of methane cannot be thermogenic but a mixture of surface diffusion and thermogenic methane containing gas bubbles cannot be excluded.

Conclusions

We conclude that the major contributions to the enhanced atmospheric methane levels are produced in the upper levels of the water column. We cannot exclude an ebullitive source or thermogenic methane however, from an isotopic mass balance argument it is clear that the majority of the methane must come from the surface waters. And we further argue that it is locally produced and not transported laterally nor advectively.

The two distinct layers with light $\delta^{13}C\text{-}CH_4$ signals, that we see several times, also indicate either two different source regions that either are due to different processes or that the sources are tied to migrating biota.

Future Studies

There are numerous ways to take this further. The most obvious would be to:

1. To further test the amount of ebullition taking place.by a series of benthic bubble traps. To better understand to what extent sediment ebullition takes place, its composition, and its spatial and temporal variability. Both in general and at the ebullition sites.
2. Secondly, it would be necessary to utilise a current profiler while retrieving BBL water samples in the future if we want to be able to make predictions based on turbulence-theory.
3. It would be interesting to use RNA to get a better understanding of the active microbials communities in the water column. To find out which methanogenic pathways are active, when, and where.
4. To expand the isotope evidence by studying both δD as well as $\delta^{13}C$.

Acknowledgements

There are many people who aided me during this project and to whom I am in debt. First and foremost, I would like to take time to give thanks to my supervisor Volker Brüchert for his support and for spending his time on our many extended discussions. And, for giving me space to try and, sometimes (often?), fail on my own. The staff at Askölaboratoriet, Eva Lindell, Mattias Murphy, Eddie Eriksson, and Carl-Magnus Wiltén whose competence and energy contributed much to the project. I must also not forget all the staff at the Department of Geological Sciences at Stockholm University with honourable mentions to Draupnir Einarson, Arne Lif, Hildred Crill, Heike Siegmund and Richard Gyllencreutz, whom I went out of my way to trouble. I am also grateful to Rienk Smittenberg, Mikaela Holm, Johanna Waldheim and Malin Lindström for helping out with fieldwork.

Finally, I would like to extend my heartfelt thanks to the Swedish Royal Navy, particularly the captain and crew of HMS Kullen, for finding and salvaging all my equipment. Without their assistance this projected would have had to be abandoned halfway through.

Thank you all!

Bibliography

Abram, J. and Nedwell, D. (1978). Inhibition of methanogenesis by sulphate reducing bacteria competing for transferred hydrogen. *Archives of Microbiology*, 117(1), pp.89-92.

Axelsson, F., 2018, 'An investigation of methane production in oxygenated surface water during an algal bloom in the Askö area, Northern Baltic proper', bachelor thesis, Stockholm University, Stockholm.

Belles, A., Alary, C. and Mamindy-Pajany, Y. (2016), Thickness and material selection of polymeric passive samplers for polycyclic aromatic hydrocarbons in water: Which more strongly affects sampler properties? *Environ Toxicol Chem*, 35: 1708–1717. doi:10.1002/etc.3326

Berg, P., Røy, H., & Wiberg, P. L. (2007). Eddy correlation flux measurements: The sediment surface area that contributes to the flux. *Limnology and Oceanography*, 52(4), 1672–1684. doi:10.4319/lo.2007.52.4.1672

Boudreau, B. P. 2001. Solute transport above the sediment-water interface, p 104-126. In B. P Boudreau and B. B Jørgensen [eds.], The Benthic Boundary Layer: Transport Processes and Biogeochemistry. Oxford University Press.

Boudreau, B. P., Jørgensen, B. B. 2001. Introduction, p 2. In B. P Boudreau and B. B Jørgensen [eds.], The Benthic Boundary Layer: Transport Processes and Biogeochemistry. Oxford University Press.

Chen, Y., Cheng, J. and Creamer, K. (2008). Inhibition of anaerobic digestion process: A review. *Bioresource Technology*, 99(10), pp.4044-4064.

Conrad R (2005) Quantification of methanogenic pathways using stable carbon isotopic signatures: a review and a proposal. *Organ Geochem* 36: 739–752.

Boundary Exchange : Air-Water and Sediment-Water Interfaces, 2005, Conference Proceedings, Retrieved from https://www.semanticscholar.org/paper/Boundary-Exchange-%3A-Air-Water-and-Sediment-Water/fff8a9d13acf47362e4163c82257eab86dce3972?navId=paper-header 2019-01-08

Dade, B. D., A. Hogg, and B. P. Boudreau. 2001. Physics of Flow above the Sediment-Water Interface, p. 4-43. In B. P. Boudreau and B. B. Jørgensen [eds.], The Benthic Boundary Layer: Transport Processes and Biogeochemistry. *Oxford University Press*.

Damm, E., Kiene, R., Schwarz, J., Falck, E. and Dieckmann, G. (2008). Methane cycling in Arctic shelf water and its relationship with phytoplankton biomass and DMSP. *Marine Chemistry*, 109(1-2), pp.45-59.

Etiope, G. (2017). Abiotic Methane in Continental Serpentinization Sites: An Overview. *Procedia Earth and Planetary Science*, 17, pp.9-12.

Fredriksson, J. P., 2017, 'Investigating the Benthic Boundary Layer Using an Autonomous Lander in the Baltic Sea: A Proof of Concept', bachelor thesis, Stockholm University, Stockholm.

Froelich P. N., Klinkhammer G. P., Bender M. K., Luedtke N. A. et al. (1979) Early oxidation of organic matter in pelagic sediments of the eastern equatorial Atlantic: suboxic diagenesis. *Geochim. Cosmochim.* Acta 43, 1075-1090.

Fuex A. N. (1977) The use of stable carbon isotopes in hydrocarbon exploration. Geochem. Explor. 7, 155-188

Galimov, E.M., 1974.Carbon Isotopesin Oil and Gas Geology.N.A.S.A. (Natl.Aeron. Space Adm.) Washington,D.C., 1974 (Translationfrom: "Izotopy uglerodav neftegazovoygeologii", Nedra

Hays, G. (2003). A review of the adaptive significance and ecosystem consequences of zooplankton diel vertical migrations. *Hydrobiologia*, 503(1-3), pp.163-170.

Hesslein, R. H. (1976). An in situ sampler for close interval pore water studies. *Limnology and Oceanography*, 21(6), 912-914.

Holtappels, M. and Lorke, A. (2011). Estimating turbulent diffusion in a benthic boundary layer. *Limnology and Oceanography: Methods*, 9(1), pp.29-41.

Holtappels, M. 2009, 'Exchange of Nutrients and Oxygen between Sediments and Water Column: the Role of the Benthic Boundary Layer', PhD thesis, Max Planck Institute for Marine Microbiology, Bremen.

Houweling, S., F. Dentener, and J. Lelieveld, 2000: Simulation of preindustrial atmospheric methane to constrain the global source strength of natural wetlands. *J. Geophys. Res*., 105, 17243–17255.

Jakobsson, M., O'Regan, M., Gyllencreutz, R. and Flodén, T. (2016). Seafloor terraces and semi-circular depressions related to fluid discharge in Stockholm Archipelago, Baltic Sea. *Geological Society, London, Memoirs*, 46(1), pp.305-306.

Jørgensen, B. (1982). Mineralization of organic matter in the sea bed—the role of sulphate reduction. *Nature*, 296(5858), pp.643-645.

Jeffrey. Santrock, Stephen A. Studley, and J. M. Hayes, Isotopic analyses based on the mass spectra of carbon dioxide, *Analytical Chemistry* 1985 57 (7), 1444-1448 DOI: 10.1021/ac00284a060

Jørgensen, B. and Revsbech, N. (1985). Diffusive boundary layers and the oxygen uptake of sediments and detritus1. *Limnology and Oceanography*, 30(1), pp.111-122.

Kiene, P.R., Oremland, R.S., Catena, A., Miller,L.G., Capone, D., 1986. Metabolism of reduced methylated sulfur compounds in anaerobic sediments and by a pure culture of an estuarine methanogen, Appl Environ. Microbiol. 52, 1037-1045

Knox, M., Quay, P. and Wilbur, D. (1992). Kinetic isotopic fractionation during air-water gas transfer of O2, N2, CH4, and H2. *Journal of Geophysical Research*, 97(C12), p.20335.

Kreulen, R. and Schuiling, R.D., 1982. N2-CH4-C02 fluids during formation of the DSme de l'Agout, France. *Geochim. Cosmochim*. Acta, 46: 193-203.

Lampert, W. 1989. The adaptive significance of diel vertical migration of zooplankton. Funct. Ecol. 3: 21–27.

Lebedev, V. S., Ovsyannikovw. M., M~Gilevskig. A.and Bcigdanov V. M. (1969) Fraktionierun der Kohlenstoffisotope durch mikrobiologishe Prozesse in der biochemischen Zone. .4ttge*. Grol. 12, 621-24.

Liss P. S. and Slater P. G. (1974) Flux of gases across the air–sea interface. *Nature* 247, 181–184.

Lovley, D. R. and Klug, M., J., 1983. Methanogenesis from Methanol and Methylamines and Acetogenesis from Hydrogen and Carbon Dioxide in the Sediments of a Eutrophic Lake, *Applied and Environmental Microbiology*, Apr. 1983, p. 1310-1315

Lundmark, K. 2017. 'Acoustic Survey of Sea Floor Features in Asköfjärden', Bachelor thesis, Stockholm University, Stockholm

Marty, D. G. (1992). Ecology and metabolism of methanogens. In: Vially, R. (Ed.), Bacterial Gas, Editions Technip, Paris, pp 13-24.

Massey, L.K., Polyoxymethylene (acetal), in: *Permeability Properties of Plastics and Elastomers*, 2nd Ed., pp. 57– 60. William Andrew Publishing, Norwich, NY, 2nd edition, 2002.

Morimoto, S., Fujita, R., Aoki, S., Goto, D. and Nakazawa, T. (2017). Long-term variations of the mole fraction and carbon isotope ratio of atmospheric methane observed at Ny-Ålesund, Svalbard from 1996 to 2013. *Tellus B: Chemical and Physical Meteorology*, 69(1), p.1380497.

Glud, R. N., Gundersen, J. K., Jørgensen, B. B., Revsbech, N.P. and Schulz, H. D. (1994). Diffusive and total oxygen uptake of deep-sea sediments in the eastern South Atlantic Ocean:in situ and

laboratory measurements. *Deep Sea Research Part I: Oceanographic Research Papers*, 41(11-12), pp.1767-1788.

Oremland R. S. (1979) Methanogenic activity in plankton samples and in fish intestines: a mechanism for in situ methanogenesis in oceanic waters*. Limnol. Oceanogr*. 24, pp 1136–1141.

Oremland R. S. and Polcin S. (1982) Methanogenesis and sulfate reduction: Competitive and noncompetitive substrates in estuarine sediments. *Appl. Environ. Microbiol*. 44, 1270-1276.

Owens, N., Law, C., Mantoura, R., Burkill, P. and Llewellyn, C. (1991). Methane flux to the atmosphere from the Arabian Sea. *Nature*, 354(6351), pp. 293-296.

Pope, S. B. 2000. Turbulent Flows. Cambridge University Press.

Reeburgh W. S. (1980) Anaerobic methane oxidation: rate depth distribution in Skan Bay sediments. *Earth Planet. Sci. Lett. 47*, 345–352.

Ritzrau, W. and Thomsen, L. (1997). Spatial distribution of particle composition and microbial activity in benthic boundary layer (BBL) of the Northeast Water Polynya. *Journal of Marine Systems*, 10(1-4), pp. 415-428.

Sagan, C., Thompson, W., Carlson, R., Gurnett, D. and Hord, C. (1993). A search for life on Earth from the Galileo spacecraft. *Nature*, 365(6448), pp. 715-721. Sadly, cut but never forgotten.

Schoell, M., Multiple origins of methane in the earth, *Chemical Geology,71* (1988) 1-10

Schönheit P, Keweloh H, Thauer RK (1981) Factor F_{420} degradation in *Methanobacterium hermoautotrophicum* during exposure to oxygen. FEMS Microbiol Lett 12: 347–349.

Sieburth J. M. (1960) Acrylic acid, an “antibiotic” principle in Phaeocystis blooms in Antarctic waters. *Science* 132, pp 676–677.

Schmale, O., Wäge, J., Mohrholz, V., Wasmund, N., Gräwe, U., Rehder, G., Labrenz, M. and Loick-Wilde, N. (2017). The contribution of zooplankton to methane supersaturation in the oxygenated upper waters of the central Baltic Sea. *Limnology and Oceanography*, 63(1), pp.412-430.

Storz G, Tartaglia L, Farr S, Ames B (1990) Bacterial defenses against oxidative stress. Trends Genet 6: 363–368.

Stumm W. and Morgan J. J. (1981) Aquatic Chemistry. Wiley, New York, NY.

Söderberg, P. and Flodén, T. (1992). Gas seepages, gas eruptions and degassing structures in the seafloor along the Strömma tectonic lineament in the crystalline Stockholm Archipelago, east Sweden. *Continental Shelf Research*, 12(10), pp.1157-1171.

Talaia M. A. R., (2007) Terminal Velocity of a Bubble Rise in a Liquid Column, *World Academy of Science, Engineering and Technology International Journal of Physical and Mathematical Sciences* Vol:1, No:4,

Thomsen, L., Graf, G., Martens, V. and Steen, E. (1994). An instrument for sampling water from the benthic boundary layer. *Continental Shelf Research*, 14(7-8), pp.871-882.

Thomsen, L., T. van Weering, and G. Gust. 2002. Processes in the benthic boundary layer at the Iberian continental margin and their implication for carbon mineralization. *Progress in Oceanography* 52: 315-329.

Townsend, D. W., Keller, M. D., Sieracki, M. E. and Ackleson, S. O. 1992. Spring phytoplankton blooms in the absence of vertical water column stratification. - Nature 360: 59-62.

Von Karman, T. 1930. Mechanische und Ähnlichkeit und Turbulenz, p. 85-105. Proceedings of the Third International Congress of Applied Mechanics.

Wanninkhof, R. (1992). Relationship between wind speed and gas exchange over the ocean. *Journal of Geophysical Research*, 97(C5), 7373. doi:10.1029/92jc00188

Weiss, R. F., *J. Chem. Eng. Data*, 18, 235 (1971).

Welhan, J.A., 1981. Carbon and hydrogen gases in hydrothermal systems: the search for a mantle source. *Ph.D. Thesis, University of California*, San Diego, Calif., 194 pp.

Whiticar, M., Faber, E. and Schoell, M. (1986). Biogenic methane formation in marine and freshwater environments: CO2 reduction vs. acetate fermentation—Isotope evidence. *Geochimica et Cosmochimica Acta*, 50(5), pp.693-709.

Whiticar, M. (1999). Carbon and hydrogen isotope systematics of bacterial formation and oxidation of methane. *Chemical Geology*, 161(1-3), pp.291-314.

Wiesenburg, Denis & Guinasso, Norman. (1979). Equilibrium solubilities of methane, carbon monoxide, and hydrogen in water and sea water. *Journal of Chemical & Engineering Data*. 24. 356. 10.1021/je60083a006.

Woolf D. K. (1997) Bubbles and their role in air–sea gas exchange. In The Sea Surface and Global Change (eds. P. S. Liss and R. A. Duce). Cambridge University Press, pp. 173–205.

Xiao, K. Q., Beulig, F., Kjeldsen, K. U., Jørgensen, B. B., & Risgaard-Petersen, N. (2017). Concurrent methane production and oxidation in surface sediment from Aarhus Bay, Denmark. *Frontiers in microbiology*, 8, 1198.

Yamamoto, S., Alcauskas, J. B., Crozier, T. E., J*. Chem. Eng. Data*, 21, 78 (1976).

Zheng, Y., Harris, D., Yu, Z., Fu, Y., Poudel, S., Ledbetter, R., Fixen, K., Yang, Z., Boyd, E., Lidstrom, M., Seefeldt, L. and Harwood, C. (2018). A pathway for biological methane production using bacterial iron-only nitrogenase. *Nature Microbiology*, 3(3), pp.281-286.

acta est fabula plaudite

Appendix

$\delta^{13}C$ response relative to peak area for the GC/Isolink IRMS

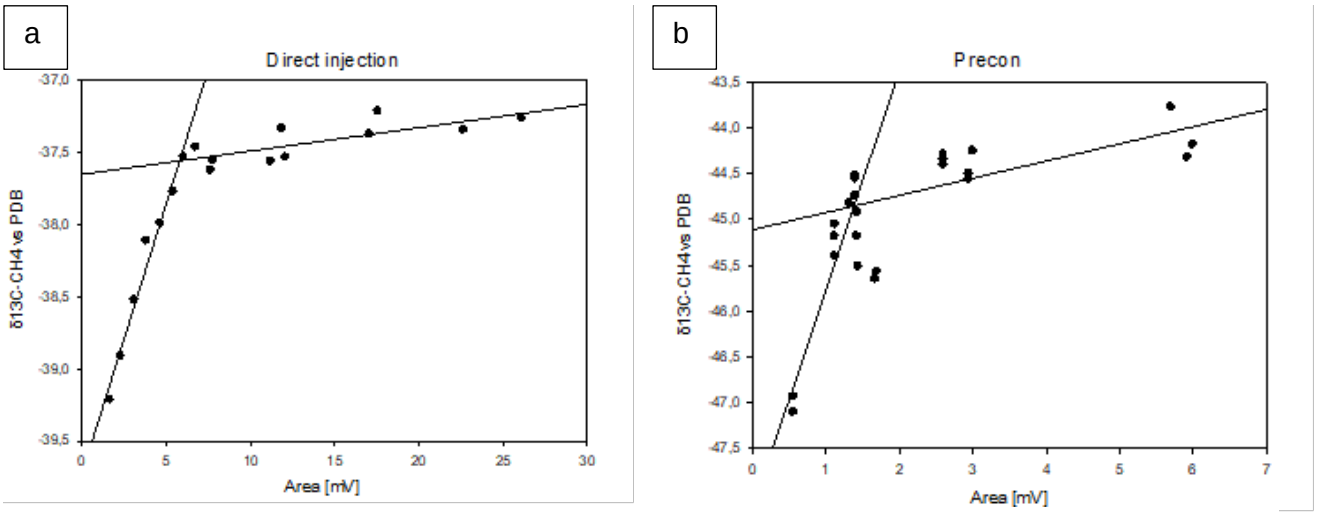

Figure Appendix 1: The isotope fractionation given by using a standard for a) direct injection or b) PreCon.

Comments regarding the deployments.

2017-11-26

The lander had recently had the elevator engine replaced and its waterproof housing improved. A glitch in the battery charger cable had been fixed. These fixes were performed just prior to the deployment and there was not enough time to test the equipment beforehand. So, it was decided to just test the Hesslein sampler. And collect long term benthic CTD data

2018-02-XX

Deployment was planned but rapid growth of sea ice the days prior made it impossible to reach the intended sampling destination. Sampling cancelled.

2018-04-XX

As a cost cutting act two sampling expeditions was planned for the same boat trip. Lander deployment and core retrieval for Johanna Waldheim's bachelor thesis. Cores were retrieved, the lander deployed and water sampling in progress when an erratic ice floe was spotted drifting in from the north. It was decided that the risk of further ice floes drifting into the lander buoy was too big a hazard. Water sampling was discontinued, and the lander was retrieved from the seafloor.

2018-05-17

Perfect weather. Calm and sunny. All sampling objectives achieved. Upon returning to retrieve the equipment, on June 11, it was found that the buoy marking the spot was missing. And it was unclear whether the lander was still on the seafloor without its marker or completely lost. The RS Electra was immediately called in to do a preliminary sweep of the area with its multibeam but with negative results. The following weekend a new multibeam search was performed, also with negative results. After exploring the options regarding how to find the equipment a query requesting assistance was sent to The Royal Navy. On July 11th the minesweeper HMS Kullen performed a sweep of the area, localised, and salvaged the equipment. All equipment was retrieved in working albeit somewhat haggard condition. All scientific data, except data from the Hesslein sampler was salvaged.

2018-08-06

All objectives achieved.

2018-08-16

All sampling objectives achieved except the benthic bubble trap which was not deployed. Upon retrieval it was discovered that rust had affected the grip of the transmission from the elevator engine to the shaft driving the elevator. As a result, the grip was not strong enough to lift the elevator. Instead it had run down into the sediments. Long term BBL CTD data lost. This was a direct result of the wear and tear imposed upon the benthic lander during its 8 weeks lost at sea. Time constraints had made it impossible to perform proper maintenance.

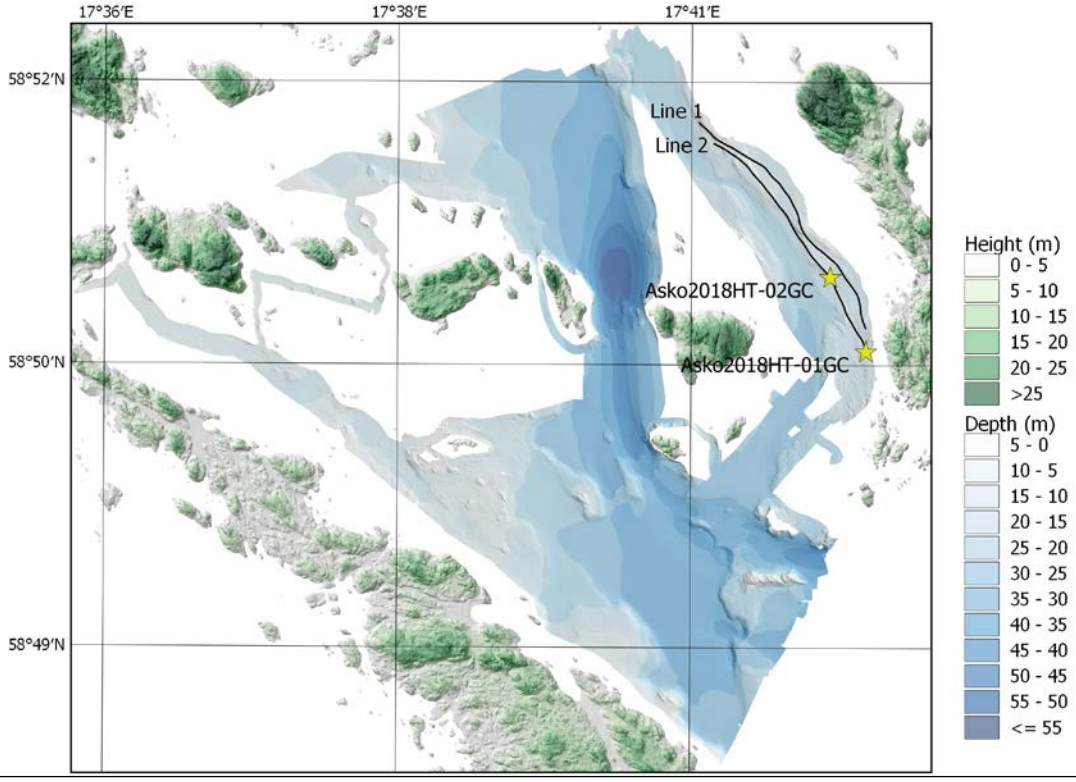

Figure Appendix 2: Bathymetry of the studied region. Data collected by R/V Electra. Courtesy of Richard Gyllencreutz (personal communication).

Core Incubation

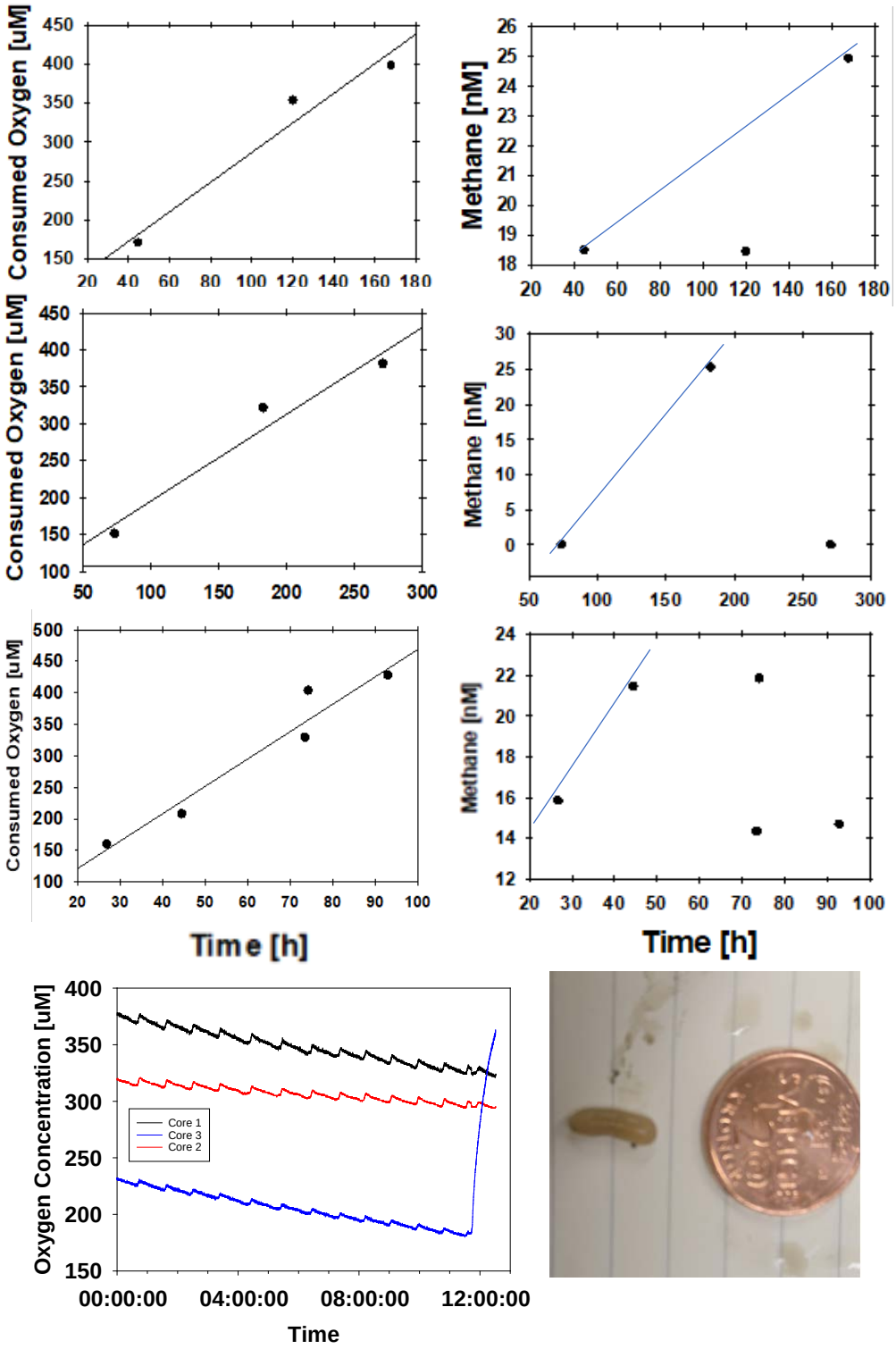

Figure Appendix 3: Results of the core incubation experiment. The oxygen concentrations followed a general trend with the resets, but the methane concentrations varied. The oxygen consumption was higher in one core which was found to be due to the actions of a Halycryptus spinolusosus.

Discussing a Failed Core Incubation Experiment

One of the major reasons of doing core incubations is to measure how a solute builds up with time. By comparing this to the oxygen consumption rate a flux can be calculated. From this perspective the core incubation experiment was a failure. No trend in accumulation of methane could be detected. This could be due to two reasons: 1) The sampling of the water allowed for uncontrolled mixing of the sampled water with the surrounding baseline water or 2) the samples were stored untreated for too long and degraded. Both are possible. The samples were stored, un-poisoned, for some time before analysis. The possibility of water mixing was known a priori but it was deemed to be less of a problem than removing the core and emptying it outside of the incubating water. One such sampling attempt was tried, and it was not possible to restore the core, since the uppermost sediments were so easily disturbed, without creating large amounts of suspended particles. However, the core incubation experiment clearly highlighted a massive problem which is that of scaling. The three cores exhibit distinctly different respiration rates with core 1 respiring faster than core 2 and 3 combined. This is for cores collected at the same time within a 0.5 m^2 area. It seems that the elevated consumption of core 1 was due to the actions of one specimen of Halicryptus spinulosus which was found in the core. It has also been shown that the benthic fauna, in the same region, changes dramatically during the year. This throws a massive spanner into the works and seriously questions the validity of using respiration rates from core incubations as representative, scalable, and well defined for seemingly homogenous sediments. Indeed, this is where a method with lower resolution such as high resolution close to sediment-water interface water samples from the benthic boundary layer can be of use instead.

Search for the lost lander

Search with RV Electra

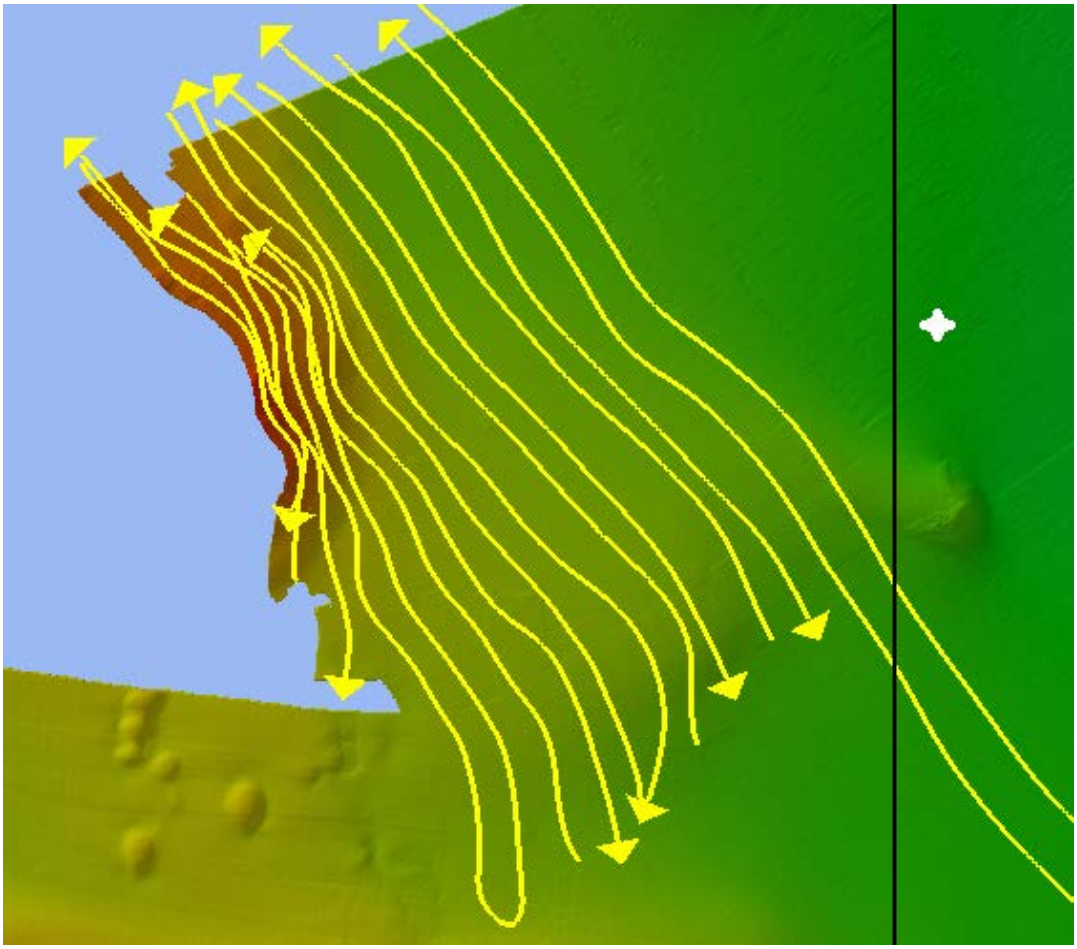

Figure 1. The yellow line show where RS Electra searched with her multibeam. The white mark is where it was subsequently found by HMS Kullen of the Royal Navy.

Underlag för eftersök. Beskrivining av utrustning och position där den försvann.

Landaren är en ca 2 meter hög ställning av aluminium. Från ställningen löper ett rep där vi fäst flytkulor några meter ovanför landaren och längst upp på repet (vid ytan) sitter en boj. Bojen är märkt med Stockholms Universitet, Volker Brüchert och hans telefonnummer (076-1352542). Vi satte ner landaren vid koordinaterna 58 51.3786 N 017 39.1373 E den 17:e maj kl 15.30. Vädret vid nedsättningen var lugnt men vi kunde inte uppmäta strömhastigheten. Vid tidigare tillfällen har strömhastigheten vid botten varit i storleksordningen 1-5 cm/s. Landaren sattes på 26 meters djup. Planen var att hämta landaren måndag den 11:e juni och det var då vi insåg att den var borta. Eller åtminstonde att bojen som markerade dess position var borta. Vi sökte av området genom att köra några transekter med R/V Elektra af Askö men har inte sett något på hennes multibeam. Landaren själv kan vara svår att se på multibeam men repet den är markerad med har några flytkulor för att minska dess effektiva vikt (vi vill inte att den ska sjunka för djupt i sedimenten) som borde synas väldigt bra. Vår hypotes har varit att bojen som markerade hennes position antingen blivit stulen (har tydligen varit ett problem tidigare för Östersjöcentrum) eller att repet fastnat i en passerande båt och att landaren släpats bort en bit. Den är så tung att man måste ha en kranbåt för att kunna lyfta upp den så vi tror inte att den är stulen.

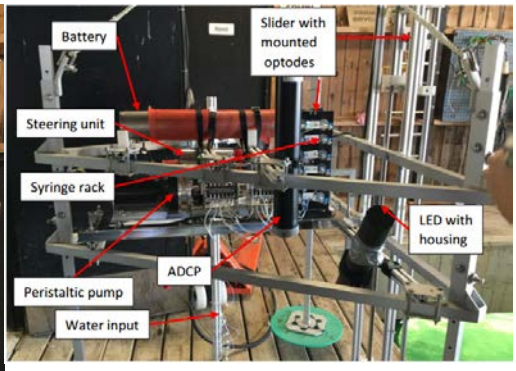

När landaren är full-lastad väger den runt 100 kg. Vi monterar flytkulor på repet några meter ovanför landaren för att reducera dess effektiva vikt i vattnet. Med dem så är den inte tyngre (i vattnet) än att man kan lyfta den med en arm.

Figure 2. Bentisk landare med utrustning.

Den bentiska landaren består av en ram tillverkad av profilerade fyrkantsrör i aluminium. På ramen har vi sen monterat en hiss driven av en liten motor i en PVC(?)-tryckbehållare. På hissen har vi fäst en CTD (Sea and Sun Technology, ej med på bild)och extra syreoptoder (Aandera NO). Vi har också ett kamerasystem bestående av en GoPro-kamera och en LED ljuskälla som båda är monterade i cylindriska tryckbehållare. Vi har en 12-kanals peristalitskpump kopplade från intag nära havsbotten till sprutor monterade på en ställning för att kunna ta vattenprover med hög spatialupplösning nära botten. Hissen, pumpen, och optoderna är kopplade till en styrenhet i en tryckbehållare av titan som i sin tur är kopplad till en litiumjonbatteri som också sitter i en tryckbehållare. Vi har också monterat en ADCP (AquaDoppCurrentProfiler) som är monterad nedå och mäter strömhastigheten med hög spatial upplösning närmast botten. Den är akustisk och mäter dopplerskiftet hos partiklar som flyter med strömmen. Vid den senaste nedsättningen hade vi även monterat på en bubbelfälla (en tratt med en slang kopplad till en exetainer). Batteriet som styr hissen, pumpen etc börjar bli gammalt och vi räknar med att det har batteritid för 2-3 veckor. Batteriet som styr den autonoma ADCP:n är hemmabyggt och som ADCP:n var programmerad så borde det ha räckt ca 2 veckor.

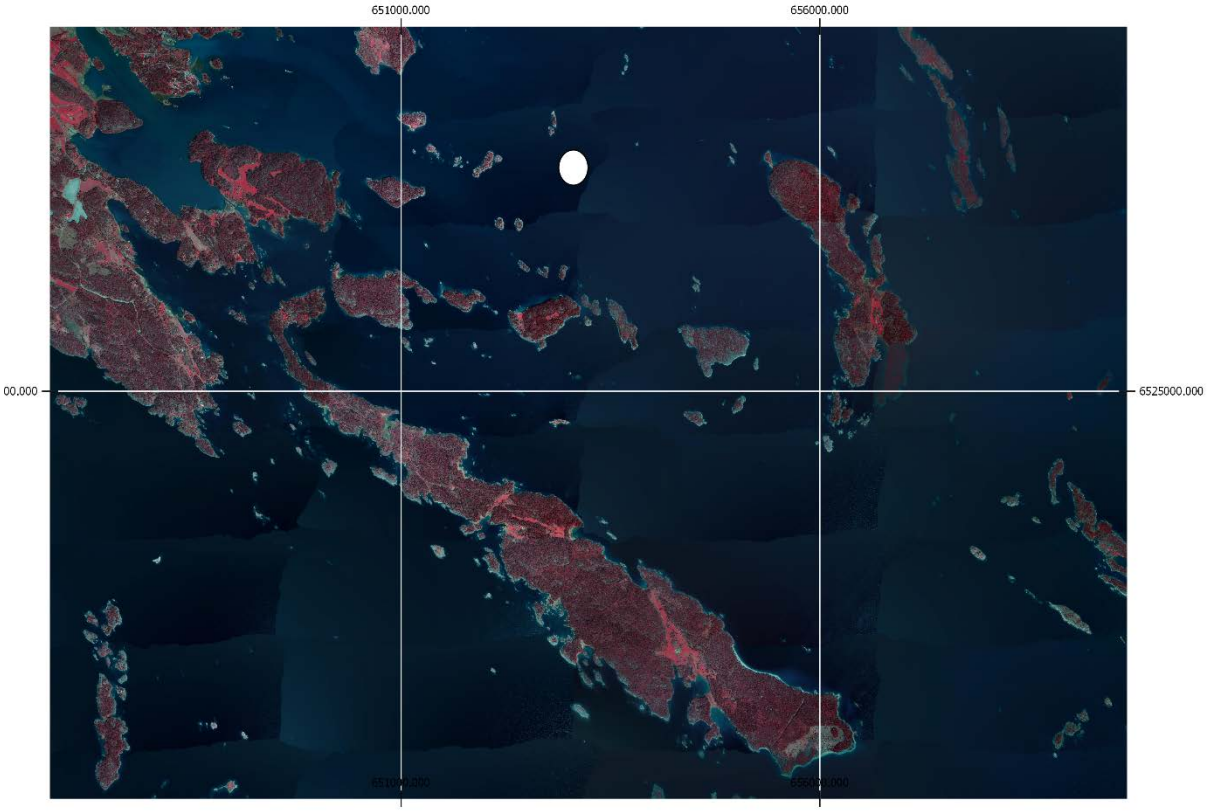
651000.000
656000.000
00.000
6525000.000

FÖRSVARSMAKTEN
FJÄRDE SJÖSTRIDSFLOTTILJEN
HMS KULLEN

Datum 2018-07-13 | Beteckning Rapport | Sida 1 (1)

Rapport efter bärgning av mätutrustning tillhörande Stockholms Universitet.

Bakgrund:
Inkommen förfrågan 2018-06-21 via METOCC om hjälp av lokalisering och om möjligt bärgning av mätutrustning tillhörande Stockholms Universitet (SU).

Genomförande:
2018-07-11 – kl 1110: HMS Kullen påbörjar sök i området FIFÅNGSDJUPET med utgångspunkt från angiven position i underlag (5851.3786N 01739.1373E). Sökningen genomfördes inledningsvis i en radie 100 meter runt utgångspositionen.

2018-07-11 – kl 1200: Identifieringsdyk med ROV genomförs på vad som bedöms vara objektet på POS 5851.4033N 01739.1974E dvs ca 75 meter NO om angiven position. Objektet visar sig mycket riktigt vara mätutrustningen vilken står upprätt på botten och bedöms bärningsbart.

*2018-07-11 – kl 1325:*Mätutrustningen bärgas med hjälp av bärgningskrok och ROV.

Anmärkning:
Av de tre bojar som fästs vid mätutrustningen så var en punkterad och den tamp som fästs i dessa gick ej att använda vid bärgningen och kapades därför. Bojarna samt tamp medföljde vid återlämningen.

Mätutrustningen fördes till Berga örlogsbas där den hämtas av personal från SU under fredagen den 13 juli 2018.

Örlkn Johan Grönhaug
Fartygschef HMS Kullen